Impulsive excitation of coherent magnons and phonons by subpicosecond laser pulses in the weak ferromagnet FeBO₃

A. M. Kalashnikova,[1,2] A. V. Kimel,[1] R. V. Pisarev,[2] V. N. Gridnev,[2] P. A. Usachev,[2] A. Kirilyuk,[1] and Th. Rasing[1]

[1]*IMM, Radboud University Nijmegen, 6525 ED Nijmegen, The Netherlands*
[2]*A. F. Ioffe Physico-Technical Institute, Russian Academy of Sciences, 194021 St. Petersburg, Russia*

Coherent magnons and phonons are excited by subpicosecond laser pulses in the weak ferromagnet FeBO₃. Impulsive stimulated Raman scattering (ISRS) is proven to be the microscopic mechanism of the excitation. It is shown that coherent magnons can be excited by both linearly and circularly polarized laser pulses where the efficiency of the process depends on the mutual orientation of the magnetic and crystallographic axes and the light propagation direction. The strong ellipticity of the ferromagnetic magnon mode is demonstrated, both experimentally and theoretically, to be essential for the excitation and observation of such coherent magnons. Because of this ellipticity, the amplitude of the coherent magnons excited by linearly polarized light may exceed by 2 orders of magnitude the amplitude of those excited by circularly polarized light. The primary difference between the excitation of coherent magnons by linearly polarized pulses via ISRS and via the earlier reported process of photoinduced magnetic anisotropy is discussed. Furthermore, the ISRS process is found to be responsible for the excitation of two optical phonon branches (8.4 and 12.1 THz) observed in our experiments. A coherent excitation, with a temperature-independent frequency of 0.7 THz, has also been observed in the magnetically ordered phase but could not be assigned to any optical phonon modes known in FeBO₃. The well-pronounced dependence of the amplitude of this mode on temperature suggests that this mode of nonmagnetic origin becomes Raman active only in the magnetically ordered phase and, therefore, can be excited and observed only below the Néel temperature.

PACS number(s): 78.20.Ls, 75.40.Gb, 42.65.Dr, 75.50.Ee

I. INTRODUCTION

The experimental and theoretical aspects of the interaction of subpicosecond laser pulses with magnetically ordered media are topics of great current interest, both from a fundamental point of view as well as because of potential applications.[1] Already the first observation of ultrafast (within 0.1 ps) light-induced demagnetization in nickel films[2] suggested that a conventional thermodynamical approach to the problem is not justified.[3–5] New theoretical models have to be worked out in order to understand recent results such as ultrafast light-induced demagnetization,[2,4–12] phase transitions,[13,14] magnetic-order sensitive excitation of phonon modes,[15] generation of a magnon squeezed state,[16] excitation of coherent spin precession,[17–25] and the magnetization reversal by a single 40 fs laser pulse.[26] The theoretical models proposed so far to explain these exciting experimental observations[27–34] leave several important issues open for further discussion.

One of these issues is related to the actual time scale within which spins response to the action of an ultrashort laser pulse.[7,9,10,33,34] In view of this, two types of responses of a magnetic system can be recognized. The first type can only occur in absorbing media and consists of *indirect* mechanisms in which the spin system changes in response to one or another type of photoinduced perturbation in the medium, not related itself to the spin degree of freedom. This can be an increase in electron temperature, destroying magnetic order, a photoinduced electronic transfer between different ion sites, modifying magnetocrystalline anisotropy, etc. The verification of the time scales of these processes is often complicated because of the several cross-interacting

subsystems (photons, thermalized and nonthermalized electrons, phonons, and spins)[6] involved, which are characterized by their own response times.

Another type of mechanism can be referred to as *direct*, where the perturbation of the spin system takes place during the light pulse via optical transitions directly. These latter mechanisms are, therefore, extremely sensitive to the light polarization, which provides the possibility to control their efficiency. The optical spin orientation in semiconductors is an example of such mechanism.[35] In metals and dielectrics, however, experimental studies of such mechanisms on the subpicosecond time scale are rare.[16,23–25,36] On a longer time scale, the possibility to change the magnetization of a medium via polarization-sensitive optical transitions has been known since the 1960s, when a helicity-dependent light-induced magnetization was predicted[37,38] and observed[39] in a transparent paramagnetic medium subjected to 30 ns circularly polarized pulses. This phenomenon was named the inverse Faraday effect. Further attempts to observe light-induced magnetization in a magnetically ordered medium were reported in Ref. 40, where, however, only heat-induced effects on the magnetization were most probably detected.[41]

Recently, the excitation of spin precession by circularly polarized 100 fs laser pulses was observed[23] in the weak ferromagnetic orthoferrite DyFeO₃. The phase of the spin precession was defined by the helicity of the laser pulses. It was shown that the impact of circularly polarized laser pulses could be seen as the action of an effective light-induced magnetic field directed along the wave vector of light. This effect, referred to as an *ultrafast* inverse Faraday effect, was assumed not to have any particular requirements for the medium apart from possessing a large magneto-

optical susceptibility. Later, supporting this idea, similar effects were observed in ferrimagnetic garnet films[24] as well as in thin films of the amorphous metallic alloy GdFeCo.[25]

The combination of direct and indirect mechanisms is of practical interest because it could lead to the control of the magnetic state by light, as shown experimentally in Ref. 26, where a helicity-dependent switching of the magnetization by 40 fs circularly polarized pulses was observed in a metallic film. Thus, a complete understanding of the processes taking place during and after the optical excitation by a sub-picosecond laser pulse is of particular importance. The present paper is therefore devoted to the experimental and theoretical study of the direct mechanisms of the excitation of coherent spin precession triggered by laser pulses in a transparent medium.

As was already proposed in the 1960s,[42,43] the excitation of coherent processes in a transparent medium, such as lattice vibrations (coherent phonons) or spin precession (coherent magnons or spin waves), might occur via stimulated Raman scattering. It was shown in the beginning of the 1980s that *impulsive* stimulated Raman scattering (ISRS) leads to efficient excitation of acoustic phonons via picosecond pulses.[44–46] The development of mode-locked femtosecond lasers has since then resulted in a large number of experimental and theoretical works contributing to a substantial progress in the field of ultrafast light-matter interactions (for reviews see Refs. 47–50). In view of the current interest in ultrafast spin dynamics, the generation of coherent magnons via impulsive stimulated Raman scattering is an intriguing option. Indeed, second-order ISRS was shown to be the mechanism for the generation of a magnon squeezed state.[16] However, only recently first-order stimulated Raman scattering was suggested as the mechanism for the experimentally observed coherent magnon generation.[23] An unambiguous demonstration of the generation of coherent magnons via first-order ISRS in $FeBO_3$ was reported in Ref. 52. The strong ellipticity of the magnon modes appeared to be crucial for this observation, as we show in the present paper. The specific role of the magnetic properties of the medium in this ISRS process was already pointed out in a general phenomenological theory worked out in Ref. 53.

In this paper we present comprehensive experimental and theoretical results on coherent magnon excitation in $FeBO_3$ and discuss the particular role of the magnon mode ellipticity in this process, utilizing a phenomenological theory of ISRS. Alternatively, the action of light pulses on a magnetic medium is described by light-induced effective fields, which excite a coherent spin precession. We show that in the case of a multisublattice medium such as $FeBO_3$, several effective fields must be taken into account. This yields an adequate description of the action of laser pulses on a magnetic system even when the changes in the latter are large and the problem becomes strongly nonlinear.

The choice of the weakly ferromagnetic $FeBO_3$ (Ref. 54) is motivated by two reasons. On the one hand, $FeBO_3$ is characterized by a magnetic structure with "easy-plane" magnetic anisotropy and strong ellipticity of the spin precession,[55] the influence of which can be readily detected in experiments. On the other hand, $FeBO_3$ is characterized by large values of the magneto-optical coefficients. In addi-
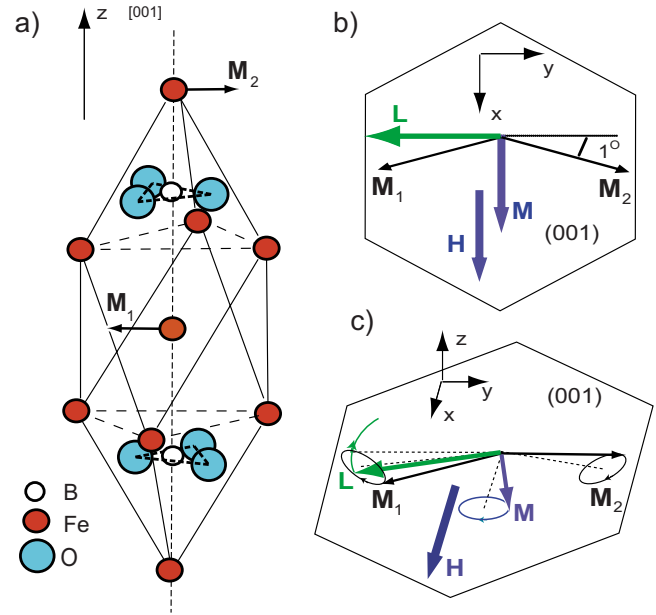

FIG. 1. (Color online) (a) Schematic representation of (a) crystallographic structure of $FeBO_3$ (Ref. 56), (b) magnetic structure in the *xy* plane, and (c) quasiferromagnetic resonance mode (Ref. 58). $M_{1,2}$ are magnetic moments of two iron sublattices and **M**, **L**, and **H** are ferromagnetic vector, antiferromagnetic vector, and applied magnetic field, respectively. Note that the length of **L** and the canting of $M_{1,2}$ are not to scale.

tion, lots of information on the magneto-optical properties and on spontaneous Raman and Brillouin light scattering for this compound are available.[56,57]

The paper is organized as follows. Section II is devoted to the description of the crystallographic and static magnetic structure of $FeBO_3$ (Sec. II A) and to the properties of the spin precession in this material (Sec. II B). An analysis of the symmetry of the optical and magneto-optical properties is given in Sec. II C. In Sec. III we describe the excitation of coherent magnons by impulsive stimulated Raman scattering using the equation of motion for the magnon normal coordinates. In Sec. IV we present the experimental results of the pump-probe experiments on laser-induced generation of spin precession in $FeBO_3$ and discuss them on the basis of theory developed in Sec. III. In Sec. V we consider the same experimental results in terms of light-induced effective fields and the Landau-Lifshitz (LL) equation. The relevant features arising from the presence of several magnetic sublattices are considered. The agreement between this approach and the one of Sec. III is discussed. Section VI is devoted to the generation of coherent optical phonons in $FeBO_3$ via ISRS, while Sec. VII presents the conclusions.

II. EASY-PLANE WEAK FERROMAGNET $FeBO_3$

A. Crystallographic and magnetic structure

Iron borate $FeBO_3$ crystallizes in the rhombohedral calcite-type crystallographic structure (space group: $R\bar{3}c$) with 2 f.u. per unit cell as shown in Fig. 1(a).[54,56,59] The Fe^{3+} ions occupy identical octahedrally coordinated positions.[60]

Below the Néel temperature T_N=348 K, the magnetic moments $\mathbf{M}_1$ and $\mathbf{M}_2$ of the two Fe^{3+} sublattices are coupled antiferromagnetically. It is common to describe this magnetic structure in terms of the ferromagnetic vector $\mathbf{M}=\mathbf{M}_1+\mathbf{M}_2$ and the antiferromagnetic vector $\mathbf{L}=\mathbf{M}_1-\mathbf{M}_2$, as shown in Fig. 1(b). In terms of these vectors the Hamiltonian describing the magnetic structure of $FeBO_3$ for a homogeneous case has the form[61]

$$\mathcal{H} = \frac{A}{2}\mathbf{M}^2 + \frac{b}{2}L_z^2 + \frac{a}{2}M_z^2 - D[\mathbf{M}\times\mathbf{L}]_z - \mathbf{M}\mathbf{H}. \quad (1)$$

Often the parameters of the magnetic structure are given in terms of effective fields $\mathbf{H}^{\mathrm{eff}}=-\partial\mathcal{H}/\partial\mathbf{M(L)}$. The first term in Eq. (1) describes the isotropic exchange interactions and corresponds to an effective exchange field, $H_E=A|\mathbf{M}|=2.6\times 10^3$ kOe.[62] The second and third terms describe the magnetocrystalline anisotropy. The constants a and b are positive, which corresponds to an easy-plane type of spin alignment, where spins of both sublattices are perpendicular to the crystallographic z axis. The effective magnetocrystalline anisotropy field is $H_A\simeq 1.7$ kOe.[62] The presence of the fourth term in Eq. (1) accounts for the antisymmetric exchange interactions,[63,64] leading to a canting of the spins in the xy plane. The effective Dzyaloshinskii field is $H_D\simeq 61.9$ kOe,[62] corresponding to a canting angle of $\sim H_D/H_E\simeq 1°$ and a net magnetic moment of $4\pi M_s=115$ G at $T=300$ K (Ref. 65) (238 G at $T\to 0$ K). The magnetocrystalline anisotropy in the xy plane is as weak as $H_{A'}\simeq 0.26$ Oe.[62] Therefore, a magnetic field of up to 0.5 kOe applied in the xy plane was sufficient to saturate the samples.

B. Dynamic magnetic properties

In general, the precession of a magnetic moment $\mathbf{M}_i$ around its equilibrium position defined by intrinsic and applied fields is described by the LL equation.[66] In the case of $FeBO_3$, comprised of two magnetic sublattices, the spin precession is usually described as the precession of the ferromagnetic $\mathbf{M}(t)$ and antiferromagnetic $\mathbf{L}(t)$ vectors [Fig. 1(c)], for which the LL equations have the form[57,67]

$$\frac{d\mathbf{M}(t)}{dt} = -\gamma\{[\mathbf{M}(t)\times\mathbf{H}^{\mathrm{eff}}]+[\mathbf{L}(t)\times\mathbf{h}^{\mathrm{eff}}]\}+\mathbf{R}_M; \quad (2a)$$

$$\frac{d\mathbf{L}(t)}{dt} = -\gamma\{[\mathbf{M}(t)\times\mathbf{h}^{\mathrm{eff}}]+[\mathbf{L}(t)\times\mathbf{H}^{\mathrm{eff}}]\}+\mathbf{R}_L, \quad (2b)$$

where γ is the gyromagnetic ratio. The effective fields $\mathbf{H}^{\mathrm{eff}}$ and $\mathbf{h}^{\mathrm{eff}}$ include the internal and applied magnetic fields and are defined as the gradients $\mathbf{H}^{\mathrm{eff}}=-\partial\mathcal{H}/\partial\mathbf{M}$ and $\mathbf{h}^{\mathrm{eff}}=-\partial\mathcal{H}/\partial\mathbf{L}$ of Hamiltonian (1) with respect to the corresponding vectors. The terms $\mathbf{R}_{M(L)}$ account for the damping of the precession amplitude of $\mathbf{M}$ and $\mathbf{L}$, respectively. Below we neglect the damping terms because they do not play any role in the discussion.

The two eigensolutions of the linearized equations [Eqs. (2a) and (2b)] give two spin precession modes existing in $FeBO_3$, with the frequencies[58,68,69]

$$\Omega^{\mathrm{FMR}} = \gamma\sqrt{H(H+H_D)+2H_E H_{A'}}, \quad (3a)$$

$$\Omega^{\mathrm{AFMR}} = \gamma\sqrt{H_D(H+H_D)+2H_E H_A}. \quad (3b)$$

Equation (3a) describes the frequency Ω^{FMR} of the low-energy quasiferromagnetic resonance[70] (FMR) mode [Fig. 1(c)]. This is a homogenous precession of the magnetic moments of the two sublattices in such a way that the angle between them does not change. Equation (3b) represents the high-energy quasiantiferromagnetic resonance (AFMR) mode. In this mode the angle between the sublattice magnetic moments varies. The ferromagnetic and antiferromagnetic vectors can be represented as a sum of static $\mathbf{M}^{(0)}$ and $\mathbf{L}^{(0)}$ and time-dependent $\mathbf{m}(t)$ and $\mathbf{l}(t)$ components,

$$\mathbf{M}(t) = \mathbf{M}^{(0)} + \mathbf{m}(t), \quad (4a)$$

$$\mathbf{L}(t) = \mathbf{L}^{(0)} + \mathbf{l}(t). \quad (4b)$$

In these terms the ferromagnetic resonance (FMR) mode involves oscillations of the l_x, m_y, and m_z components of $\mathbf{l}(t)$ and $\mathbf{m}(t)$, while the antiferromagnetic resonance (AFMR) mode involves time variations of the m_x, l_y, and l_z components.

The FMR mode is characterized by strong ellipticity[55] because the in-plane magnetocrystalline anisotropy is very weak compared to the out-of-plane one. For a magnetic field applied in the easy plane of magnetic anisotropy along the x axis, the ratios between the out-of-plane and in-plane deviations of the spins are[58]

$$\frac{m_z}{l_x} = \frac{\Omega^{\mathrm{FMR}}}{2\gamma H_E}, \quad \frac{m_z}{m_y} = \frac{\Omega^{\mathrm{FMR}}}{2\gamma H_D}. \quad (5)$$

For moderate magnetic fields around $H=10$ kG, this gives $m_z/l_x\sim 0.01$ and $m_z/m_y\sim 0.4$. The ellipticity of the AFMR mode is, in turn,[58]

$$\frac{l_z}{m_x} = \frac{\Omega^{\mathrm{AFMR}}}{2\gamma H_E} \quad (6)$$

and is smaller by 1 order of magnitude than for the FMR mode.

C. Magneto-optical properties

In the spectral range of the Ti:sapphire laser (central photon energy $E_0=1.54$ eV) $FeBO_3$ is characterized by a low absorption, which is related to the electric-dipole forbidden d-d transition $^6A_{1g}\to {}^4T_{1g}$ centered at 1.4 eV.[60,71] The absorption coefficient for $E_0=1.54$ eV is $\alpha=80$ cm^{-1}.[8] The main contribution to the refractive index in this region stems from the allowed charge-transfer transition located above 2.9 eV.[72]

$FeBO_3$ is an optically uniaxial crystal with the optical axis parallel to the crystallographic z axis. The dielectric permittivity tensor in the paramagnetic phase has only two nonvanishing components $\varepsilon_{xx}^0=\varepsilon_{yy}^0\neq\varepsilon_{zz}^0$. At the photon energy $E_0=1.54$ eV $FeBO_3$ is characterized by a strong crystallographic birefringence $\Delta n=n_x-n_z=0.08$.[72]

Below T_N the interaction of light with the medium can be described phenomenologically in terms of contributions to the dielectric permittivity tensor $\hat{\varepsilon}$ caused by the presence of magnetic order. It is convenient to decompose ε_{ij} into anti-

TABLE I. The equilibrium magnetic contributions to the dielectric permittivity tensor ε_{ij} (column 2) and its modulation by FMR and AFMR spin precessions (columns 3 and 4) linear in the spin deviations. Underlined are the components used in the discussion of the FMR mode excitation via ISRS. The coordinate axes x, y, and z are chosen as shown in Fig. 1. The external magnetic field **H** is assumed to be along the x axis, so that $\mathbf{L}^{(0)} \| y$, $\mathbf{M}^{(0)} \| x$.

Tensor element	Static $(\mathbf{l}(t)=0, \mathbf{m}(t)=0)$	FMR[a] $(l_x, m_y, m_z \neq 0)$	AFMR[a] $(m_x, l_y, l_z \neq 0)$
ε_{xx}^s	$b_2 L_y^2 + c_1 M_x L_y$	0	$b_2 L_y l_y + b_5 L_y l_z + c_8 M_x l_z$
ε_{yy}^s	$b_1 L_y^2 - c_2 M_x L_y$	0	$b_1 L_y l_y - b_5 L_y l_z - c_8 M_x l_z$
ε_{zz}^s	$b_3 L_y^2 + c_4 M_x L_y$	0	$b_3 L_y l_y + c_4(M_x l_y + m_x L_y)$
$\underline{\varepsilon_{xy}^s}$	0	$\underline{(b_1-b_2)l_x L_y} - \frac{1}{2}(c_1+c_2)(M_x l_x - m_y L_y) + c_3 L_y m_z$	0
ε_{xz}^s	0	$\underline{2b_4 l_x L_y} + c_5(m_y L_y - M_x l_x) - c_6 L_y m_z$	0
ε_{yz}^s	$-b_4 L_y^2 + c_5 M_x L_y$	0	$b_6 L_y l_z + c_7 M_x l_z$
ε_{xy}^a	0	$iK m_z$	0
$\underline{\varepsilon_{xz}^a}$	0	$iK_1 \underline{m_y + iK_2 l_x}$	0
ε_{yz}^a	$iK_1 M_x - iK_2 L_y$	0	$iK_1 m_x - iK_2 l_y$

[a]Full expressions accounting for the second-order contributions are given in Appendix A.

symmetric $\varepsilon_{ij}^a = -\varepsilon_{ji}^a$ and symmetric $\varepsilon_{ij}^s = \varepsilon_{ji}^s$ parts,[73] which are, according to the Onsager principle, odd and even with respect to the (anti)ferromagnetic vectors, respectively. These contributions are presented in column 2 of Table I. This table contains only the magnetic contributions relevant for our experimental geometry, where the magnetic field **H** and ferromagnetic vector **M** are along the x axis and the antiferromagnetic vector **L** is along the y axis.

In the spectral region around $E_0 = 1.54$ eV, where absorption is weak and can be neglected, the antisymmetric part ε_{ij}^a of the dielectric permittivity tensor is purely imaginary.[74] ε_{ij}^d defines the value of the magnetic circular birefringence or Faraday effect.[75] FeBO$_3$ is characterized by a high value of the Faraday rotation that can reach $5000°/$cm close to the absorption edge in the green part of the spectrum.[65,76] Since $\varepsilon_{xy}^a = 0$, observation of the Faraday effect is possible only for light with a wave vector having a finite angle with the z axis. However, in the latter case the rotation of the light polarization caused by the Faraday effect is strongly quenched by the crystallographic birefringence. The interplay between these two effects leads to drastic changes in the resulting rotation of the polarization plane, depending on the angle between the wave vector and the z axis.[76] The rotation of the light polarization plane ϕ_F is shown in Fig. 2(a) for the photon energy $E = 1.54$ eV and for an angle of incidence of $10°$ as a function of the magnetic field applied along the x axis [see inset of Figs. 2(a) and 2(b)]. Taking into account the crystallographic birefringence $\Delta n = 0.08$ we found that for the given angle of incidence such a rotation of the polarization plane corresponds to an intrinsic Faraday rotation of $456°/$cm, in agreement with results of Ref. 69.

The symmetric part ε_{ij}^s is purely real if absorption is neglected in the spectral region around $E_0 = 1.54$ eV. It is an even function of **M** and **L** and defines the value of the magnetic linear birefringence (MLB) or Voigt effect.[75] Although it is a second-order effect with respect to the magnetic-order parameters, in magnetically ordered media the MLB can be comparable with the first-order Faraday effect.[77,78] Figure

2(c) shows the MLB measured for light propagating along the z axis [inset of Figs. 2(c) and 2(d)]. The temperature dependencies of the Faraday rotation and MLB are presented in Figs. 2(b) and 2(d), respectively.

An additional modulation of the dielectric permittivity tensor occurs in the presence of coherent spin precession. The components of ε_{ij} modulated by the FMR and AFMR precessions and linear in spin deviations are shown in columns 3–4 of Table I. In the discussion below we restrict ourselves only to the components that are linear in the small deviations m_k and l_k ($k=x,y,z$) of the (anti)ferromagnetic vectors from the equilibrium positions. Then from Table I one can see that the FMR spin precession contributes only to the off-diagonal components $\delta\varepsilon_{xy}^s$, $\delta\varepsilon_{xz}^s$, $\delta\varepsilon_{xy}^a$, and $\delta\varepsilon_{xz}^a$ of the dielectric permittivity tensor (see also Ref. 57), while the
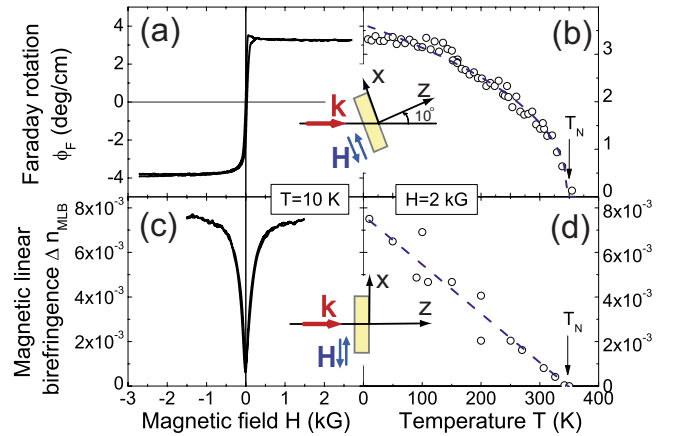

FIG. 2. (Color online) The static Faraday rotation ϕ_F as a function of (a) an applied magnetic field H and (b) temperature. The inset in the upper panels shows the experimental geometry used for Faraday rotation measurements. The magnetic linear birefringence (MLB) Δn_{MLB} as a function of (c) an applied magnetic field H and (d) temperature. The inset in the lower panels shows the experimental geometry used for MLB measurements. The dashed lines in (b) and (d) are guides for the eyes.

AFMR mode manifests itself in the $\delta\varepsilon_{xx}^s$, $\delta\varepsilon_{yy}^s$, $\delta\varepsilon_{yz}^s$, and $\delta\varepsilon_{yz}^a$ components.

III. COHERENT MAGNON EXCITATION BY SHORT LASER PULSES

A. Equation of motion for magnon normal coordinates

The possibility of exciting coherent lattice vibrations (coherent phonons) and spin precession (coherent magnons) by light was considered in Refs. 42 and 43. The process of stimulated Brillouin or Raman scattering, when a photon of energy $\hbar\omega_i$ is scattered in a medium into a photon of energy $\hbar\omega_s$, involves the creation of a phonon or magnon with energy $\hbar\Omega_0 = \hbar(\omega_i - \omega_s)$. If the scattering is triggered by short laser pulses with a spectral width significantly larger than the frequency of the phonon (or magnon), both photons with energies $\hbar\omega_i$ and $\hbar\omega_s$ involved in the scattering process are contained in the laser pulse, resulting in an ISRS process.[45] The electric-dipole transitions involved in the ISRS process cannot change the spin quantum numbers. Therefore, for the creation of coherent magnons via ISRS, spin-orbit interactions in the excited state are required.

Extensive theoretical and experimental studies of excitation of coherent phonons via ISRS were performed by several groups (for reviews see Refs. 46, 48, and 49). However, in the case of a magnetically ordered medium lacking time-inversion symmetry, new features in the ISRS are expected, as described in Ref. 53.

In this section we consider the excitation of coherent spin precession by laser pulses using an approach, where the light is described by a classical electric field E and the coherent excitation in the medium is described by the normal coordinate Q. In the case of a magnon, Q describes the precessional motion and is complex. This is in contrast to the case of phonons, where the normal coordinates describe ion displacements and are therefore real variables. For the FMR precession mode Q is introduced (see Appendix B) in the following way:[79]

$$\begin{bmatrix} l_x(t) \\ m_y(t) \\ m_z(t) \end{bmatrix} = 2\,\mathrm{Re}\left[Q(t) \begin{pmatrix} ia_x \\ ib_y \\ b_z \end{pmatrix} \right], \tag{7a}$$

$$a_x = \sqrt{2\gamma\mathcal{M}_0}\sqrt{\frac{\gamma H_E}{\Omega_0}}, \quad b_z = \frac{1}{2}\sqrt{2\gamma\mathcal{M}_0}\sqrt{\frac{\Omega_0}{\gamma H_E}}, \tag{7b}$$

$$b_y/a_x = -M_x^{(0)}/L_y^{(0)}, \quad b_z/a_x = \Omega_0/2\gamma H_E, \tag{7c}$$

$$l_x(t) = ia_x(Q - Q^*),$$

$$m_y(t) = ib_y(Q - Q^*),$$

$$m_z(t) = b_z(Q + Q^*), \tag{7d}$$

where $\mathcal{M}_0$ is the sublattice magnetization and $\Omega_0 = \Omega^{\mathrm{FMR}}$ is the frequency of the FMR mode. $Q(t)$ describes the coherent magnons in the time domain, while $\{ia_x, ib_y, b_z\}$ describe the

magnon polarization. The real values a_x, b_y, b_z are chosen in such a way that the Hamiltonian describing the coherent FMR magnons has a simple form,

$$\mathcal{H}_{\mathrm{magnon}} = \Omega_0 Q(t) Q^*(t). \tag{8}$$

The interaction of a laser pulse with a transparent magnetic medium is described in general by the Hamiltonian,

$$\mathcal{H}_{\mathrm{int}} = -\frac{\delta\varepsilon_{ij}}{16\pi}\mathcal{E}_i(t)\mathcal{E}_j^*(t), \tag{9}$$

where $\mathcal{E}_i(t)$ is the time-dependent amplitude of the electric field of light, $\mathbf{E} = \mathrm{Re}\,\mathcal{E}(t)e^{i\omega t}$.

The Hamiltonian equation of motion for the system described by $\mathcal{H} = \mathcal{H}_{\mathrm{magnon}} + \mathcal{H}_{\mathrm{int}}$ has the form[80,81]

$$i\frac{\partial Q}{\partial t} = \frac{\partial\mathcal{H}}{\partial Q^*}, \tag{10}$$

which can be easily transformed into the equation

$$\frac{dQ}{dt} + i\Omega_0 Q = -i\frac{\partial\mathcal{H}_{\mathrm{int}}}{\partial Q^*}. \tag{11}$$

When optical absorption is significant, the Hamiltonian $\mathcal{H}_{\mathrm{int}}$ [Eq. (9)] is not valid[82] and the more general equation holds,

$$\frac{dQ}{dt} + i\Omega_0 Q = -iF(t), \tag{12}$$

where the form of the driving force $F(t)$ depends on the type of process leading to the magnon excitation.

In general, Eq. (12) is not restricted to the case of ISRS only. When ISRS in a transparent medium is considered, the driving force behaves like $|E(t)|^2$ and can be approximated by a delta function $\delta(t)$ in the time domain. If absorption is present laser action can in addition exert a quasistationary driving force, which can be approximated by a Heaviside step function. The latter would correspond to a non-Raman process of magnon excitation. Moreover, for the case of light-induced coherent phonon excitation it was shown theoretically and experimentally that in an absorbing medium a combination of resonant Raman scattering and non-Raman (displacive) processes has to be considered.[51,83]

B. Optical excitation of coherent magnons in a transparent medium

In the spectral region where absorption can be neglected, the interaction of laser pulses with a medium has an instantaneous character. In this case, in the equation of motion for magnons [Eq. (11)] the driving force exerted by laser pulses is impulsive,

$$\frac{\partial Q}{\partial t} + i\Omega_0 Q = -i\frac{I_0}{4nc}\frac{\partial\varepsilon_{ij}}{\partial Q^*}e_i e_j^*\delta(t), \tag{13}$$

where I_0 is the integrated pulse intensity, e_i is a component of the light polarization unit vector, n is the refraction index, and c is the speed of light. The dispersion of $\delta\varepsilon(\omega)$ can be neglected in Eq. (13), since the magnon frequency $\Omega_0 = \omega_i - \omega_s \ll \omega_0$ (the central pump frequency) and we consider a medium with low absorption.

We consider two directions of the pump pulse propagation. The pump beam propagates along the optical z axis in the first case and along the y axis in the second one. In both cases the magnetic field **H** is applied in the easy plane of magnetic anisotropy along the x axis. As shown below, the excitation of coherent magnons in these two cases is significantly different.

1. Excitation of magnons by optical pulses with wave vector perpendicular to the easy plane of magnetic anisotropy

To describe the interaction of the pump pulses propagating along the z axis with the medium one has to consider the components $\delta\varepsilon_{xy}^{a}$ and $\delta\varepsilon_{xy}^{s}$ of the dielectric permittivity tensor. We find the main contributions to $\varepsilon_{xy}^{a(s)}$ caused by the magnons using Table I [Eq. (7d)] and taking into account that $L_{y}^{(0)} \gg M_{x}^{(0)}$, $l_{x} \gg m_{z}$,

$$\delta\varepsilon_{xy}^{a} = -\delta\varepsilon_{yx}^{a} = iKm_{z} = iKb_{z}(Q + Q^{*}), \quad (14a)$$

$$\delta\varepsilon_{xy}^{s} = \delta\varepsilon_{yx}^{s} \approx GL_{y}^{(0)}l_{x} = iGL_{y}^{(0)}a_{x}(Q - Q^{*}), \quad (14b)$$

where $G = b_{1} - b_{2}$ in the notation used in Ref. 52.

In the case of circularly polarized light $\sigma^{\pm}$ the contribution from the symmetric part $\delta\varepsilon^{s}$ of the dielectric permittivity vanishes and the solution of Eq. (13) has the following form (see Appendix C):

$$Q^{\sigma^{\pm}}(t) = \pm \frac{1}{8nc}Kb_{z}I_{0}[\sin\Omega_{0}t + i\cos\Omega_{0}t], \quad (15a)$$

$$m_{z}^{\sigma^{\pm}}(t) = \pm \frac{1}{4nc}Kb_{z}^{2}I_{0}\sin\Omega_{0}t, \quad (15b)$$

$$l_{x}^{\sigma^{\pm}}(t) = \pm \frac{1}{4nc}Kb_{z}a_{x}I_{0}\cos\Omega_{0}t, \quad (15c)$$

where the $\pm$ signs correspond to the opposite senses of helicity of the circularly polarized pump pulses. This result is, in general, consistent with that of Ref. 23, where a helicity-dependent spin precession excitation was observed and stimulated Raman scattering was proposed as a possible microscopic mechanism.

For light linearly polarized at an angle θ with respect to the y axis, the contribution from the antisymmetric part $\delta\varepsilon_{xy}^{a}$ vanishes and the solution of Eq. (13) has the form (see Appendix C)

$$Q^{\text{lin}}(t) = \frac{1}{8nc}GL_{y}^{(0)}a_{x}I_{0}\sin 2\theta[-\cos\Omega_{0}t + i\sin\Omega_{0}t], \quad (16a)$$

$$m_{z}^{\text{lin}}(t) = -\frac{1}{4nc}GL_{y}^{(0)}b_{z}a_{x}I_{0}\sin 2\theta\cos\Omega_{0}t, \quad (16b)$$

$$l_{x}^{\text{lin}}(t) = -\frac{1}{4nc}GL_{y}^{(0)}a_{x}^{2}I_{0}\sin 2\theta\sin\Omega_{0}t, \quad (16c)$$

showing that the initial phase and amplitude of the excited coherent magnons can be controlled not only by the helicity of the circularly polarized laser pulses but also by the azimuthal angle θ of the linearly polarized pulses. Note that the amplitudes of the spin precession excited by circularly and linearly polarized lights are defined by the first- and second-order magneto-optical susceptibilities K and G, respectively. In the magnetically ordered solids these susceptibilities can be comparable in magnitude.[77,78]

2. Excitation of magnons by optical pulses with a wave vector parallel to the antiferromagnetic vector

To describe the interaction of the pump pulses propagating along the y axis with the medium one has to consider the components $\delta\varepsilon_{xz}^{a}$ and $\delta\varepsilon_{zx}^{a}$ of the dielectric permittivity tensor. Taking into account the ellipticity of the spin precession,[55] Eq. (7d), and the ratio between L_{y}^{0} and M_{x}^{0} we obtain

$$\delta\varepsilon_{xz}^{a} = -\delta\varepsilon_{zx}^{a} = i(K_{1}m_{y} + K_{2}l_{x}) = (K_{1}b_{y} + K_{2}a_{x})(Q - Q^{*}), \quad (17a)$$

$$\delta\varepsilon_{xz}^{s} = \delta\varepsilon_{zx}^{s} \approx 2b_{4}L_{y}^{(0)}l_{x} = i2b_{4}L_{y}^{(0)}a_{x}(Q - Q^{*}). \quad (17b)$$

Therefore, the magnons excited by linearly and circularly polarized lights are described as follows (see Appendix C):

$$Q^{\text{lin}}(t) = \frac{1}{4nc}b_{4}L_{y}^{(0)}a_{x}I_{0}\sin 2\theta[-\cos\Omega_{0}t + i\sin\Omega_{0}t], \quad (18a)$$

$$Q^{\sigma^{\pm}}(t) = \mp \frac{1}{8nc}(K_{1}b_{y} + K_{2}a_{x})I_{0}[-\cos\Omega_{0}t + i\sin\Omega_{0}t], \quad (18b)$$

$$m_{z}^{\text{lin}}(t) = -\frac{1}{2nc}b_{4}L_{y}^{(0)}a_{x}b_{z}I_{0}\sin 2\theta\cos\Omega_{0}t, \quad (18c)$$

$$l_{x}^{\text{lin}}(t) = -\frac{1}{2nc}b_{4}L_{y}^{(0)}a_{x}^{2}I_{0}\sin 2\theta\sin\Omega_{0}t, \quad (18d)$$

$$m_{z}^{\sigma^{\pm}}(t) = \pm \frac{1}{4nc}(K_{1}b_{y} + K_{2}a_{x})b_{z}I_{0}\cos\Omega_{0}t, \quad (18e)$$

$$l_{x}^{\sigma^{\pm}}(t) = \pm \frac{1}{4nc}(K_{1}b_{y} + K_{2}a_{x})a_{x}I_{0}\sin\Omega_{0}t. \quad (18f)$$

C. Optical excitation of coherent magnons in an absorbing medium

If the absorption in the medium is considerable one cannot express the driving force exerted by laser pulse as a delta function. Instead, in analogy with the case of coherent phonon excitation,[48,84] the driving force can be of nonimpulsive character. The experimental evidence of such type of processes can be found in Refs. 21 and 24 where 100 fs laser pulses were reported to induce a quasistationary change in the magnetocrystalline anisotropy. Absorption (e.g., by im-

purity centers[21]) is involved in this process and the driving force is described by a Heaviside *step function*. Equation (12) gets the form

$$\frac{\partial Q}{\partial t} + i\Omega_0 Q = \begin{cases} -iF_0, & t > 0 \\ 0, & t < 0, \end{cases} \quad (19)$$

where F_0 can be complex in general (see Appendix C). Such type of processes can be referred to as *displacive* excitation of coherent magnons (DECMs). The solution of this equation is given in Appendix C. If, for example, Re $F_0 = 0$ and Im $F_0 \neq 0$, then

$$Q(t) = iF_0 \frac{e^{-i\Omega_0 t} - 1}{\Omega_0}, \quad (20a)$$

$$m_z(t) = 2F_0 b_z \frac{\sin \Omega_0 t}{\Omega_0}, \quad (20b)$$

$$l_x(t) = 2F_0 a_x \frac{[1 - \cos \Omega_0 t]}{\Omega_0}. \quad (20c)$$

Note that the spin precession excited via ISRS or DECM is characterized by a radically different time behavior. Namely, terms with a *cosinelike* time dependence only appear for the case of ISRS [Eqs. (15c), (16b), (18c), and (18e)], indicating that right after the excitation by the light pulse, spins are out of their equilibrium positions, which is never the case for DECM [Eqs. (20a)–(20c)]. Moreover, in the case of ISRS the spins precess around their original equilibrium directions, as depicted by the *sinelike* time dependence of $l_x(t)$ [Eq. (16c)]. In contrast, the DECM mechanism leads to a spin precession around "new" equilibrium direction generated by the light pulse. The $1 - \cos \Omega_0 t$ dependence is therefore expected for $l_x(t)$. This allows one to distinguish between these two mechanisms in the experiment.

IV. EXPERIMENTAL RESULTS AND DISCUSSION

A. Experiment

The optically excited spin precession in $FeBO_3$ was studied by means of a magneto-optical pump-probe technique.[85] The amplified laser pulses, with a duration $\tau = 150$ fs, central photon energy $E_0 = 1.54$ eV, power $P = 800$ μJ/pulse, and a repetition frequency of $\gamma = 1$ kHz from a Ti:sapphire laser, were split into a pump beam and a much less intense probe beam. The probe pulses could be delayed with respect to the pump ones by $\Delta\tau = 0 - 3$ ns. The polarization of the pump pulses was linear or circular, being controlled by half- and quarter-wave plates. The probe pulses were linearly polarized. The pump beam was focused onto a spot of about 100 μm in diameter on the sample. The probe beam was focused onto a somewhat smaller spot within the pump spot. The angle of incidence for the probe beam was 10°, while the pump beam was at normal incidence. Two experimental geometries were used: the magnetic field was always applied along the x axis, while the pump pulses were propagating along either the z or the y axis (see Sec. III B).

The spin precession induced by the pump pulses leads to a perturbation of the dielectric permittivity tensor (see Sec.
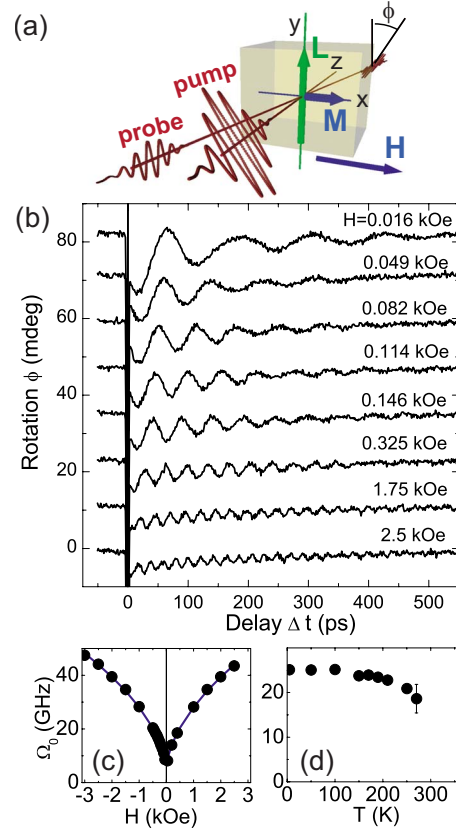

FIG. 3. (Color online) Excitation and detection of the ferromagnetic mode of spin precession by linearly polarized pump pulses. (a) Experimental geometry. (b) Pump-induced rotation of the probe polarization ϕ as a function of time delay between linearly polarized pump and probe pulses for different values of the applied magnetic field. (c) The frequency Ω_0 of the observed oscillations as a function of the applied field strength H (symbols) and its fit using Eq. (3a) (solid line). (d) The frequency Ω_0 of the oscillations as a function of temperature T. The results were obtained for a pump intensity of 10 mJ/cm². Pump pulses were linearly polarized with azimuthal angle $\theta = 45°$. Results in (b) and (c) are obtained at a temperature $T = 10$ K.

II C) which, in turn, leads to a change in the polarization of the probe beam via the Faraday effect or magnetic linear birefringence. By measuring the rotation of the probe polarization as a function of the time delay between pump and probe pulses, we can monitor the pump-induced spin precession in the time domain. Note that in a typical optical pump-probe experiment in transmission, only spin waves with very small wave vectors $k < 10^{-2}$ cm^{-1} are excited and detected because the excitation spot is large. Therefore we consider only spin waves with $k = 0$, i.e., homogeneous spin precession.

B. Detection of the light-induced FMR mode of spin precession

The rotation of the probe polarization as a function of time delay between pump (propagating along the z axis) and probe pulses is shown in Fig. 3(b) for different values of the applied magnetic field. Clear field-dependent oscillations are

observed in these data. In Fig. 3(c) the dependence of the oscillation frequency on the magnetic field is plotted. This dependence is in good agreement with the behavior of the FMR mode [Fig. 1(c)], which is described by Eq. (3a). Similarly, the dependence of the frequency of the oscillations on temperature [Fig. 3(d)] is consistent with the temperature behavior that one would expect for the FMR mode.[56,69] Our experimental data thus clearly show that the 150 fs laser pulses propagating along the z axis excite the FMR mode of coherent spin precession in $FeBO_3$.

The FMR mode supposes, as described in Sec. II B, oscillations of the l_x, m_y, and m_z components of $\mathbf{l}(t)$ and $\mathbf{m}(t)$. There are various magneto-optical effects that can serve as a probe of such a precession. That is, in the experimental geometry shown in Fig. 3(a), the spin precession may lead to a transient rotation of the probe polarization via both the Faraday effect and the MLB. For instance, $m_z(t)$ can be detected using the Faraday effect with the probe polarization rotation $\phi(t)$ equal to

$$\phi_F(t) = \omega_0 d \frac{\delta\varepsilon^a_{xy}(t)}{n} = \omega_0 d \frac{Km_z(t)}{n}, \quad (21)$$

where ω_0 is the pulse central frequency, d is the sample thickness, and n is the refractive index. In turn, $l_x(t)$ oscillations cause MLB, which also leads to a rotation of the probe polarization,

$$\phi_{MLB}(t) = \omega_0 d \frac{\delta\varepsilon^s_{xy}(t)}{n} \approx \omega_0 d \frac{GL^{(0)}_y l_x(t)\cos 2\xi}{n}, \quad (22)$$

where $G = b_1 - b_2$ is the magneto-optical coefficient (see Table I) and ξ is the incoming polarization of the probe pulse. A straightforward way to distinguish these two contributions to the rotation of the probe polarization is to study their dependence on ξ. In the case of the Faraday effect, the incoming polarization does not affect the measured signal $\phi(t)$. In contrast, in the case of MLB the signal should possess a dependence on ξ with a 180° period. In order to distinguish between the Faraday effect and MLB, we have performed measurements in the experimental geometry shown in Fig. 4(b). The probe beam was propagating along the z axis and, thus, the effect of the crystallographic birefringence on the measured signal was minimized. In Fig. 4(a) the rotation of the probe polarization is shown as a function of the time delay between pump and probe pulses for various orientations of the incoming probe polarization ξ. A clear 180° dependence of the signal on ξ is observed [Figs. 4(a) and 4(c)]. This indicates that the measured signal originates from the transient MLB [Eq. (22)] and reveals an in-plane motion of the antiferromagnetic vector $\mathbf{L}$. The fact that MLB dominates over the Faraday effect is caused by the strong ellipticity of the FMR mode of spin precession; since the magneto-optical constants K and G are comparable for the photon energy $E = 1.54$ eV, the ratio between the transient Faraday effect and MLB is mainly defined by the ratio of the dynamic components of magnetic vectors m_z/l_x and is expected to be as small as 0.01 [see Eq. (5)].
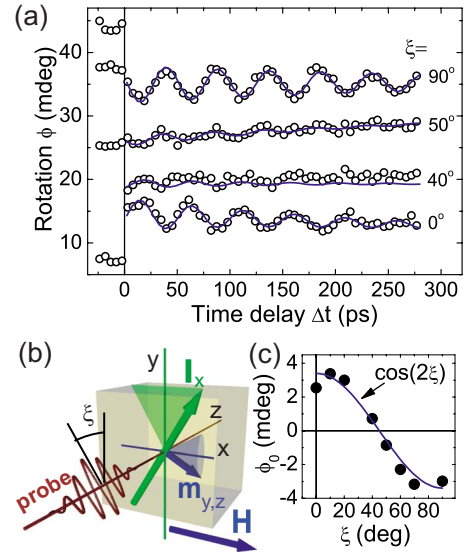

FIG. 4. (Color online) (a) The pump-induced probe polarization rotation $\phi(t)$ as a function of the time delay between pump and probe pulses measured for different initial probe polarization ξ for the experimental geometry shown in (b). Solid lines represent the fit using $\phi(\Delta t) = \phi_0 \sin(\Omega_0 \Delta t)$, $\Delta t > 0$. (c) Dependence of the amplitude of the oscillations ϕ_0 on the initial probe polarization ξ. The results were obtained for a temperature $T = 10$ K, pump intensity of 10 mJ/cm^2, and applied magnetic field $H = 1.75$ kOe. Pump pulses were linearly polarized with azimuthal angle $\theta = 45°$ [pump pulse is not shown in (b) for the sake of simplicity].

C. Excitation of coherent magnons by linearly and circularly polarized pump pulses

Figure 5(a) shows the spin precession excited by linearly polarized pump pulses for various azimuthal orientations of the pump polarization θ, as shown in Fig. 5(b). The spin precession amplitude clearly depends on θ [Fig. 5(c)].

The effect of circularly polarized pulses appeared to be dependent on the mutual orientation of pump propagation direction and antiferromagnetic vector $L^{(0)}_y$. As can be seen from Fig. 6(a), the circularly polarized pump pulses propagating along the z axis do excite spin precession, but changing their helicity affects neither amplitude nor the phase of the oscillations ($\phi^{\sigma^+} - \phi^{\sigma^-} = 0$). In contrast, the spin precession excited by circularly polarized pump pulses propagating along the y axis changes phase by 180° when the pump helicity of the light is reversed [Fig. 6(b)]. Previously, the excitation of coherent spin precession by circularly polarized 100 fs pulses was demonstrated in Refs. 23–25. The circularly polarized pulses were shown to act on the spins as effective magnetic-field pulses with a direction depending on the helicity. The phase of the excited precession, therefore, was controlled by the helicity of the pump pulses. The strength of this light-induced effective magnetic field was shown to be linearly dependent on the pump intensity, which was consistent with the proposed explanation in terms of the so-called ultrafast inverse Faraday effect (IFE). The IFE is determined by the same magneto-optical susceptibility that also accounts for the Faraday effect and is expected to be allowed in media of any symmetry. Therefore, the absence of
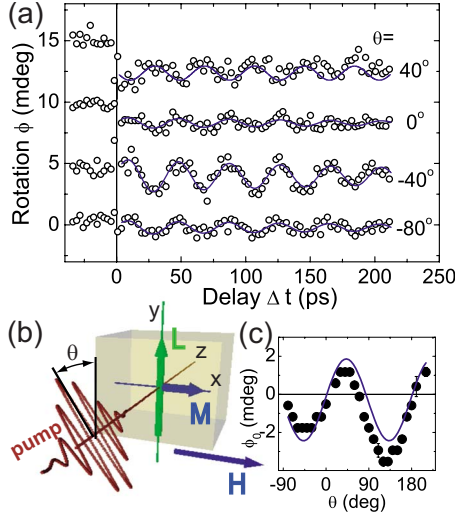
FIG. 5. (Color online) (a) The oscillations of the probe polarization as a function of the time delay between linearly polarized pump and probe pulses for different orientations of the pump polarization. The pump pulses propagate along the z axis shown in (b). The probe pulse is not shown in (b) for sake of simplicity. (c) The amplitude of oscillations as a function of the pump polarization azimuthal angle (symbols) and its fit using Eq. (23) (line). The results are obtained at $T=10$ K, $H=1.75$ kOe, and $I=10$ mJ/cm^2.

this effect in the results shown in Fig. 6(a) is, at first glance, puzzling considering the fact that the Faraday effect in FeBO$_3$ is one of the strongest among the iron oxides.[65] We note that the incompleteness of such an interpretation was pointed out in Ref. 86. Below we show that this, together with the observed polarization dependence of the excitation, can both be explained by taking into account the strongly elliptical character[55] of the spin precession modes in FeBO$_3$.[87]
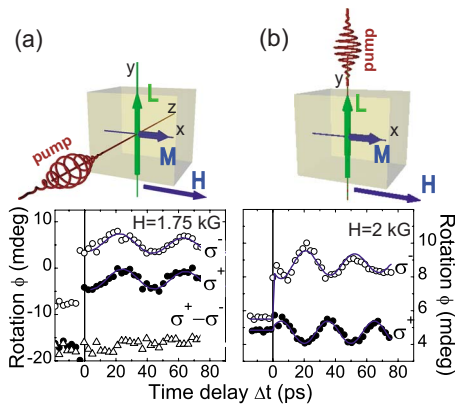

FIG. 6. (Color online) Spin precession excited by circularly polarized pump pulses propagating along (a) the z axis and along (b) the y axis. $\sigma^+ - \sigma^-$ is the difference between the spin precession amplitude excited by right- and left-handed circularly polarized pump pulses. In both cases the magnetic field is applied along the x axis and the probe is at 10° from the pump propagation direction. The results are obtained at $T=10$ K and $I=10$ mJ/cm^2.
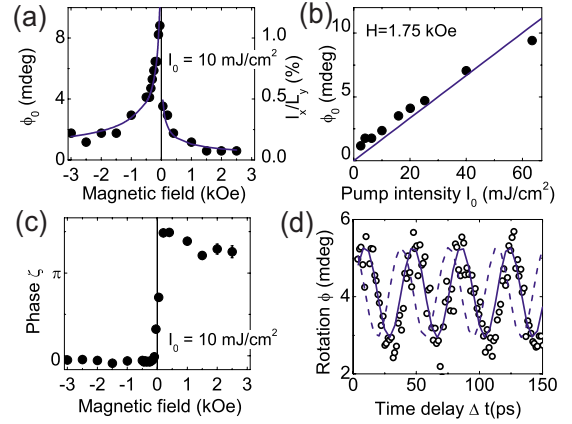

FIG. 7. (Color online) Experimental dependencies of the oscillations amplitude ϕ_0 (dots) on (a) the magnetic field H and (b) pump intensity I_0. Solid lines in (a) and (b) represent the dependencies described by Eq. (23). (c) Initial phase ζ of the pump-induced oscillations as a function of the magnetic field H when described by $\phi(\Delta t)=\phi_0 \sin(\Omega_0 \Delta t+\zeta)$. A typical experimental curve $\phi(\Delta t)$ is shown (dots) in (d). For reference, the curves $\phi(\Delta t)=\phi_0 \sin(\Omega_0 \Delta t +0)$ (solid line) and $\phi(\Delta t)=\phi_0 \sin(\Omega_0 \Delta t+\pi/2)$ (dashed line) are shown. The experimental results shown in (a)–(d) are obtained for the pump polarization $\theta=45°$ and temperature $T=10$ K.

D. ISRS as the mechanism of coherent magnon excitation

To reveal the excitation mechanism of coherent magnons in FeBO$_3$ we consider first the excitation of spin precession by the linearly polarized pump pulses propagating along the z axis [Fig. 3(a)]. Combining Eqs. (22) and (16c) for the transient rotation of the probe polarization caused by magnons excited via ISRS we obtain

$$\phi^{lin}(t) = A\frac{I_0}{4nc}GL_y^{(0)2}a_x^2 \sin 2\theta \sin \Omega_0 t, \qquad (23)$$

where $A=\omega_0 d/n$, θ is the azimuthal angle of the pump polarization, Ω_0 is the FMR frequency, $G=b_1-b_2$ is the magneto-optical coefficient (see Table I), I_0 is the integrated pump pulse intensity, ω_0 is the pump pulse central frequency, and n is the refraction index at ω_0.

Comparison of Eq. (23) with the experimental results shows good agreement. In particular, the experimentally obtained dependence of the oscillation amplitude on the applied magnetic field H [Fig. 7(a)] is described by $\phi^{lin}(H) \sim a_x^2 \sim 1/\Omega_0 \sim 1/\sqrt{H}$, following Eq. (23). The pump-induced oscillations of the probe polarization should, according to Eq. (23), possess a sinelike behavior in the time domain, which is, indeed, observed in the experiment [Figs. 7(b) and 7(d)] for the magnetically saturated sample. The theoretically predicted dependence of the oscillation amplitude on the polarization of the pump pulses $\phi^{lin}(\theta) \sim \sin 2\theta$ shows good agreement with our experimental data [Fig. 5(c)].

In the case of circularly polarized pump pulses, the transient rotation of the probe polarization excited by pulses propagating along the z and the y axes, respectively, can be expressed as

$$\phi^{\sigma^{\pm}\|z}(t) = \pm AGL_y^{(0)}a_x\left[\frac{I_0}{4nc}Kb_z\cos\Omega_0 t\right] \sim b_z a_x,$$

$$(24a)$$

$$\phi^{\sigma^{\pm}\|y}(t) = \pm AK_2\left[\frac{I_0}{4nc}(K_1 b_y + K_2 a_x)a_x\sin\Omega_0 t\right] \sim a_x^2.$$

$$(24b)$$

Now, keeping in mind that the FMR precession possesses strong ellipticity, i.e., $b_z \ll a_x$, we obtain that $\phi^{\sigma^{\pm}\|z} \ll \phi^{\sigma^{\pm}\|y} \simeq \phi^{\text{lin}\|z}$. Our experimental data (Fig. 6) show that, indeed, circularly polarized laser pulses effectively excite a helicity-dependent spin precession only when propagating along the y axis. It is worth noting that these results are in perfect agreement with the observation of spontaneous Raman scattering in FeBO$_3$ reported in Ref. 69. It was shown there that, because of spin precession ellipticity, the scattering of light propagating along the z axis is defined mainly by the second-order magneto-optical constant [i.e., by G in Eq. (23)], while the scattering of light propagating along the y axis is defined by a first-order magneto-optical constant [i.e., by K_1 and K_2 in Eq. (24b)]. Similar effect of spin precession ellipticity on the Raman-scattering intensity was reported in Ref. 88 for orthoferrites.

Here we would like to comment on the distinction between our results and those reported in Refs. 21 and 24. There the experimental observation of coherent spin precession excited by linearly polarized laser pulses in ferrimagnetic garnet films was reported. A quasistationary photoinduced change in magnetic anisotropy was proposed to be the mechanism of the excitation. Such a process can be qualified as a non-Raman process, as discussed in Sec. III C [Eq. (20)]. The oscillations of $l_x(t)$ and, consequently, $\phi(t)$ excited via such a process should obey the $(1-\cos\Omega_0 t)$-like dependence on the time delay between pump and probe pulses. In our experiment $\phi(t) \sim l_x(t) \sim \sin\Omega_0 t$ [see Figs. 3(a), 5(a), and 7(b)]. Besides, the dependence of the amplitude of the excited precession on the pump pulse intensity [Fig. 7(d)] in our experiment is different from the one observed in Ref. 21. The photoinduced change in magnetocrystalline anisotropy was suggested to be related to the absorption by impurity centers. As their concentration is limited, the dependence of the excited spin precession amplitude on the pump intensity indeed showed saturation. However, no saturation of the spin precession amplitude on the pump intensity was observed in our experiments [Fig. 7(c)].

Thus, the experimentally observed excitation of coherent magnons in FeBO$_3$ can be unambiguously described in terms of impulsive stimulated Raman scattering. The efficiency of the excitation by the pump pulses with certain polarization is defined by the ellipticity of the magnon mode, as shown theoretically in Sec. III and supported by our experimental data (Secs. IV C and IV D). It is therefore interesting and important to clarify the approach of the ultrafast inverse Faraday effect used previously to describe the light-induced spin precession in orthoferrites, garnets, and metallic alloys[89] and to compare it with our ISRS-based interpretation. For this Sec. V is devoted.

V. COHERENT MAGNON EXCITATION VIA ISRS: EFFECTIVE LIGHT-INDUCED FIELD APPROACH

The excitation of coherent spin precession by short laser pulses has been described previously using the approach, in which light acts on spins as an effective light-induced magnetic field.[89] For example, in Ref. 23 circularly polarized light pulses were suggested to act on the rare-earth orthoferrite DyFeO$_3$ as an effective magnetic field $\mathbf{H}^{\text{eff}}=K[\mathbf{E}\times\mathbf{E}^*]$, which, strictly speaking, was defined for a cubic paramagnetic medium.[90] The resulting spin precession was described by the Landau-Lifshits (LL) equation.[66] In this section we use a similar, but extended, approach based on light-induced effective fields together with the LL equation. We reveal some important features that were omitted from the considerations before,[21,23,24,31] i.e., the peculiarities of the approach when applied to a multisublattice medium. We note that the procedure presented in this section is a pictorial way to describe the driving force exerted by laser pulses on the magnetic system and is an alternative to the approach developed in Sec. III.

A. Effective fields in a multisublattice magnetic medium

To describe the impulsive action of light on the spin system, we introduce the light-induced effective fields,

$$\mathbf{H}_i^{\text{eff}} = -\frac{\partial\mathcal{H}_{i,\text{int}}}{\partial\mathbf{M}_i},$$

$$(25)$$

where $\mathbf{M}_i$ is the sublattice magnetization and $\mathcal{H}_{i,\text{int}}$ is the Hamiltonian describing the interaction of light with the ith sublattice. For the case of a one-sublattice ferromagnetic medium, the further description of the light-matter interaction is trivial because one ferromagnetic vector $\mathbf{M}$ is sufficient to describe the collective response of the magnetic system to the light action. A multisublattice magnetic medium, however, is described by several magnetic vectors $\mathbf{M}$ and $\mathbf{L}_j$, where $j=1,\ldots,n-1$ and n is the number of magnetic sublattices. Particularly, FeBO$_3$ has two magnetic sublattices with magnetizations $\mathbf{M}_1$ and $\mathbf{M}_2$. The interaction of light with each sublattice can be described by the effective field $\mathbf{H}_1^{\text{eff}}=-\partial\mathcal{H}_{1,\text{int}}/\partial\mathbf{M}_1$ and $\mathbf{H}_2^{\text{eff}}=-\partial\mathcal{H}_{2,\text{int}}/\partial\mathbf{M}_2$. Making a transition from the sublattice magnetizations to the ferromagnetic $\mathbf{M}=\mathbf{M}_1+\mathbf{M}_2$ and antiferromagnetic $\mathbf{L}=\mathbf{M}_1-\mathbf{M}_2$ vectors, one obtains two effective fields

$$\mathbf{H}^{\text{eff}} = -\frac{\partial\mathcal{H}_{\text{int}}}{\partial\mathbf{M}},$$

$$(26a)$$

$$\mathbf{h}^{\text{eff}} = -\frac{\partial\mathcal{H}_{\text{int}}}{\partial\mathbf{L}},$$

$$(26b)$$

which can also be understood as $\mathbf{H}^{\text{eff}}=\mathbf{H}_1^{\text{eff}}+\mathbf{H}_2^{\text{eff}}$ and $\mathbf{h}^{\text{eff}}=\mathbf{H}_1^{\text{eff}}-\mathbf{H}_2^{\text{eff}}$. The latter field accounts for the nonequivalent response of the Fe^{3+} ions at different crystallographic positions to the action of light. Below we show that it is this field $\mathbf{h}^{\text{eff}}$ that induces the spin precession in a weak ferromagnet. Note, that, in general, for a medium with n magnetic sublattices there are $n-1$ fields $\mathbf{h}_j^{\text{eff}}=-\partial\mathcal{H}_{\text{int}}/\partial\mathbf{L}_j$.

B. Excitation of the spin precession in FeBO₃

To describe the optical excitation of coherent spin precession we insert the effective fields (26a) and (26b) into the Landau-Lifshitz equations for a multisublattice medium [Eqs. (2a) and (2b)] and take into account the impulsive character of these fields. For the pump pulses propagating along the z axis, the Hamiltonian $\mathcal{H}_{int}$ can be found from Eq. (9) and Table I. Taking into account that $\mathbf{M}\|x$ and $\mathbf{L}\|y$ before the pulse action, we find the effective fields induced by circularly ($\sigma^\pm$) and linearly (lin) polarized pulses, as presented in Appendix D. For the excitation of the FMR mode of the coherent spin precession only the fields $\mathbf{H}^{\text{eff}}\|\hat{y}$, $\mathbf{H}^{\text{eff}}\|\hat{z}$, and $\mathbf{h}^{\text{eff}}\|\hat{x}$ are relevant,

$$\mathbf{H}^{\text{eff},\sigma^\pm} = \mp \frac{I_0}{8nc}K\delta(t)\hat{z}, \tag{27a}$$

$$\mathbf{H}^{\text{eff,lin}} = \frac{I_0}{16nc}(c_1+c_2)L_y^{(0)}\sin2\theta\delta(t)\hat{y} - \frac{1}{8nc}c_3\sin2\theta L_y^{(0)}\delta(t)\hat{z}, \tag{27b}$$

$$\mathbf{h}^{\text{eff},\sigma^\pm} = 0, \tag{27c}$$

$$\mathbf{h}^{\text{eff,lin}} = -\frac{I_0}{8nc}G\sin2\theta L_y^{(0)}\delta(t)\hat{x}. \tag{27d}$$

Therefore, the torques exerted by the pump pulses and describing the spin motion during the pulse are (see Appendix D for a full expressions)

$$\frac{dl_x^{\sigma^\pm}}{dt} = -\gamma L_y^{(0)}H_z^{\text{eff},\sigma^\pm} = \pm\gamma\frac{I_0}{8nc}KL_y^{(0)}\delta(t), \tag{28a}$$

$$\frac{dm_y^{\sigma^\pm}}{dt} = \gamma M_x^{(0)}H_z^{\text{eff},\sigma^\pm} = \pm\gamma\frac{I_0}{8nc}KM_x^{(0)}\delta(t), \tag{28b}$$

$$\frac{dm_z^{\text{lin}}}{dt} = -\gamma(M_x^{(0)}H_y^{\text{eff,lin}} - L_y^{(0)}h_x^{\text{eff,lin}}) \simeq \gamma\frac{I_0}{8nc}G\sin2\theta L_y^{(0)2}\delta(t), \tag{28c}$$

where the ratio $M_x^{(0)} \ll L_y^{(0)}$ is taken into account. Equation (27a) shows that a circularly polarized light pulse propagating along the z axis acts as an effective field $H_z^{\text{eff},\sigma^\pm}$ directed along the wave vector of light (i.e., along the z axis). This effective light-induced field exerts a torque [Eqs. (28a) and (28b)] that rotates the spins in the xy plane. When the pulse is gone (after 150 fs), the spins are out of their equilibrium orientation set by the effective fields $\mathbf{H}_E+\mathbf{H}_D+\mathbf{H}_A+\mathbf{H}_{A'}+\mathbf{H}_{\text{ext}}$. Therefore, the spins start to precess around their "old" orientations. This model is in full agreement with the results obtained in Sec. III, where circularly polarized light is shown to excite cosinelike oscillations of $l_x(t)$ [Eq. (15c)] and sinelike oscillations of $m_z(t)$ [Eq. (15b)].

In contrast to the circularly polarized pulse, the effective field $h_x^{\text{eff,lin}}$ induced by a linearly polarized light pulse [Eq. (27d)] exerts a torque [Eq. (28c)] that pushes the spins out of the xy plane. Therefore, the spin motion after the end of the

pump pulse is described by $l_x(t)\sim\sin\Omega_0 t$ and $m_z(t)\sim\cos\Omega_0 t$ [compare with Eqs. (16b) and (16c) and the experimental data in Figs. 3(b), 7(b), and 7(d)].

For the case of the pump pulses propagating along the y axis the same procedure can be followed and gives the following results for circularly polarized pulses:

$$\mathbf{h}^{\text{eff},\sigma^\pm} = \mp\frac{I_0}{8nc}K_2\delta(t)\hat{x}, \tag{29a}$$

$$\frac{dm_z^{\sigma^\pm}}{dt} = \pm\gamma\frac{I_0}{8nc}K_2L_y^{(0)2}\delta(t). \tag{29b}$$

Thus, the effect of a circularly polarized pulse propagating along the y axis resembles that of a linearly polarized one propagating along the z axis [Eq. (28c)]. Namely, the effective field induced by the former and latter pulses is h_x^{eff} and the spins move out of the xy plane during the pulse.

The presented light-induced effective fields only determine the initial spin rotations. They do not possess any dependence on the ellipticity of the FMR spin precession mode. Thus, the presence of the light-induced effective fields alone does not explain our experimental observations.

C. Role of the spin precession ellipticity

To clarify the role of the spin precession ellipticity mentioned in Sec. IV, here we present simulations of the interaction of the spin system with the pump pulses propagating along the z axis (Fig. 8), which is based on the light-induced effective fields obtained in Sec. V B. First, we consider the case of linearly polarized pump pulses. During the pulse the light-induced torque dm_z/dt [Eq. (28c)] pushes the spins out of the xy plane [Fig. 8(a)]. This results in a finite value of the dynamic component of the magnetization $m_z(\Delta t=0)$ right after the pulse. The torque dm_z/dt and, consequently, $m_z(\Delta t=0)$ are defined by the magneto-optical constant G, light intensity I_0, and polarization θ [Eq. (28b)]. When the light pulse is gone, the precessional motion of the spins toward their equilibrium position starts and after a quarter of the spin precession period the deviation of the spins is characterized by the value $l_x(\Delta t=\pi/2\Omega_0)=l_x^{\max}$ [Fig. 8(b)]. This value defines the amplitude of the signal $\phi(t)$ measured in the experiment [see Eq. (22)]. Because of the strong ellipticity of the spin precession [Eq. (5)] this deviation is 2 orders of magnitude larger than the initial one: $l_x^{\max} = (2\gamma H_E/\Omega_0)m_z(\Delta t=0) = (2\gamma H_E/\Omega_0)GI_0L_y^2$.

For the circularly polarized pulses the situation is opposite. The torque dl_x/dt created by the pump pulse rotates the spins in the xy plane, leading to a finite value $l_x(\Delta t=0)\sim KI_0L_y$ right after the pulse [Fig. 8(c)]. However, this deviation is along the direction in which the elliptical spin precession possesses the maximal amplitude. Therefore, the amplitude of the measured signal is defined by $l_x^{\max}=l_x(\Delta t=0)$ and is much weaker than the amplitude of the precession excited by the linearly polarized pump pulses: $l_x^{\sigma,\max}/l_x^{\text{lin,max}} = (\Omega_0/2\gamma H_E)K/GL_y\sim0.01$. This explains the fact that a helicity-dependent spin precession was not observed in the experiments with the pump pulses propagating along the z axis [Fig. 6(a)].
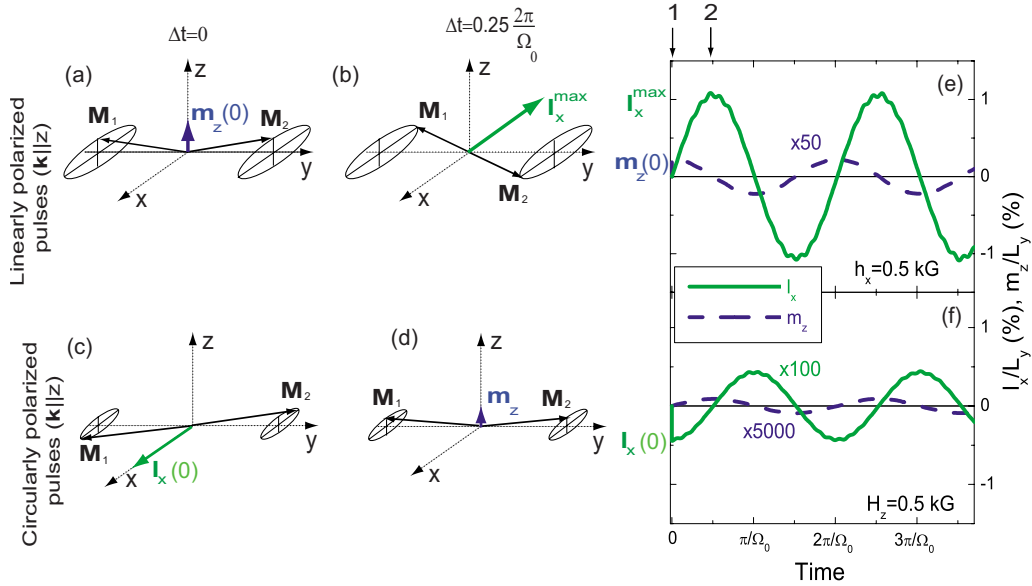
FIG. 8. (Color online) Schematic representation of the FMR precession excited by [(a) and (b)] linearly and [(c) and (d)] circularly polarized pulses propagating alone the z axis. m_z and l_x are dynamic components of the ferromagnetic and antiferromagnetic vectors. For the sake of simplicity, the ratio m_z/l_x is taken to be only 0.5 and the weak ferromagnetism is neglected, and the purely antiferromagnetic alignment is depicted. [(e) and (f)] Time dependence of l_x (green solid lines) and m_z (blue dashed lines) as obtained from the simulations (Ref. 91). During the pulse ($\Delta t=0$) the effective field induced by (a) linearly or (c) circularly polarized pulses creates the torque dm_z/dt (dl_x/dt) that pushes the spins out of (within) the xy plane. This corresponds to point 1 on the graphs (e) and (f). After the pump pulse **M** and **L** start to precess around their old equilibrium positions. Point 2 on the graphs (e) and (f) corresponds to the positions of these vectors after one quarter of the FMR period [(b) and (d)]. The maximal deviation l_x^{max} of **L** defines the amplitude of the transient probe polarization measured in the experiments. The weak high-frequency oscillations visible on graphs (e) and (f) originate from the AFMR mode.

In contrast, circularly polarized pump pulses propagating along the y axis create a torque dm_z/dt and the situation resembles the one considered above for the linearly polarized pulses, propagating along the z axis. Therefore, the amplitude of the helicity-dependent spin precession excited by circularly polarized pump pulses propagating along the y axis [Fig. 6(b)] is comparable with the amplitude of the spin precession excited by the linearly polarized ones propagating along the z axis. Note that this strong effect of the circularly polarized light originates from the effective field h_x^{eff}, directed perpendicular to the propagation direction of light, rather than from the field H_y^{eff} along the propagation direction, as one would expect at the first glance relying on the simplified model, applicable only for isotropic ferromagnetic materials. Therefore, our extended model, accounting for the two magnetic sublattices, fully addresses the comments of Ref. 86, where the simplified approach[23] was questioned.

A separate remark is required concerning the term inverse Faraday effect used in Refs. 23, 24, and 31. Following the same logic the effective fields induced by linearly polarized light can be referred to as an ultrafast inverse Cotton-Mouton or inverse Voigt effect. However, in the original papers on these phenomena,[37–39,90] the inverse Faraday effect was introduced to describe the magnetization induced in a paramagnetic medium by circularly polarized 30 ns pulses. There are several different mechanisms leading to this latter phenomenon, such as optical Stark effect and mixing different amounts of excited states into the ground state.[82] In contrast, in Ref. 23 the term ultrafast inverse Faraday effect was introduced for the effective magnetic field induced by circu-

larly polarized ultrashort laser pulses that lead to the excitation of spin precession. The microscopic mechanism of this effect is, as we show here, ISRS, in which the optical electric fields mix the ground state with excited states and create Raman coherence between the magnetic sublevels of the ground state. One should therefore be careful and keep in mind the drastic difference between the experiments with nanosecond and subpicosecond laser pulses. If the duration of the pulse is comparable with the time required for the repopulation of the different magnetic sublevels of the ground state (approximately nanoseconds), such a long excitation leads to a laser-induced magnetization not observed in the experiments with subpicosecond pulses.

Finally, we would like to note that the approaches based on the equation of motion for magnon normal coordinates (Secs. III and IV D) and on the LL equations are equivalent for the treatment of the experimental results presented in this paper. However, the latter approach will be more convenient for the description of large deviations or even switching[26] of spins caused by strong laser pulses when the equation of motion [Eq. (10)] becomes highly nonlinear.

VI. IMPULSIVE GENERATION OF COHERENT PHONONS IN FeBO₃

The spectrum of various magnetic and nonmagnetic coherent excitations in iron borate is very broad. For instance, $FeBO_3$ possesses two modes of spin precession. One of them, having a lower frequency, was successfully observed in our experiments. From the nature of the ISRS it follows
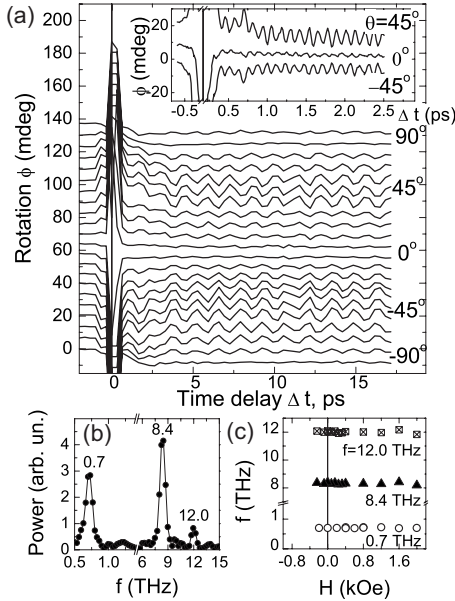
FIG. 9. (a) Transient rotation of the probe polarization as a function of the time delay between pump and probe pulses for different linear polarizations θ of the pump pulse. Inset: the signal on a shorter time scale of 0–2.5 ps. (b) Fourier spectrum of the signal measured at pump polarization $\theta=45°$. (c) Dependence of the oscillation frequency on the applied magnetic field (symbols). The results are obtained at $T=10$ K and $I=10$ mJ/cm^2.

that the highest frequency of coherent excitation that can be generated by laser pulses is limited by the pulse duration. To study the excitations in a broader spectrum, shorter laser pulses should be used. Therefore, we performed similar experiments using light pulses with a duration of 40 fs instead of 150 fs. In the case of Fourier-transform limited pulses, this change in pulse duration directly converts into an increased bandwidth and, consequently, provides access to the high-frequency excitations.

A. Experimental results

In Fig. 9(a) the transient rotation of the probe polarization, as induced by 40 fs linearly polarized laser pulses, is shown on both long (up to 15 ps) and short (up to 2.5 ps) time scales. Three modes with frequencies $f=0.7$, 8.4, and 12.0 THz are observed [Fig. 9(b)]. The frequencies of these modes are independent of the applied magnetic field [Fig. 9(c)].

The 0.7 THz frequency is approximately twice that of the antiferromagnetic resonance at room temperature.[56] However, in contrast to the behavior of the AFMR mode in FeBO$_3$,[56] this frequency does not show any noticeable dependence on temperature [Fig. 11(c)]. Therefore, we can state that the experimentally observed oscillations are not related to the antiferromagnetic mode of spin precession. This also follows from the considerations in Sec. V C that it is the ellipticity of the FMR mode which allows us to observe its excitation; the AFMR mode is characterized by an ellipticity[55] [Eq. (6)] that is 1 order of magnitude smaller than the one of the FMR mode.[56,58] We note that in spontaneous Brillouin scattering experiments[92] the intensity of the Stokes lines related to the AFMR was 2 orders of magnitude lower that those of the FMR. The frequency of 0.7 THz, however, does not coincide with any of the earlier observed five Raman-active phonon modes (A_{1g} and $4E_g$) (Refs. 93–95) or with the eight infrared-active modes.[95,96] The *ab initio* calculated spectrum of all possible phonon modes in FeBO$_3$ (Ref. 97) does not contain any mode close to 0.7 THz.

The 8.4 and 12.0 THz excitations can be attributed to the doubly degenerated Raman-active E_g optical phonon modes with frequencies 8.37 and 12.03 THz,[93,94] respectively (Fig. 10). Two infrared-active E_u modes[95,96] are close in frequency (8.03 and 12.1 THz) as well. However, in our experiments we measure a signal proportional to the finite modulation of the dielectric permittivity by phonons. The latter defines the Raman tensor and, therefore, only Raman-active modes can be detected.

B. Discussion

1. Generation of coherent phonons via ISRS

First, we discuss the excitation of the two coherent phonon modes with frequencies 8.4 and 12.0 THz. Several mechanisms of coherent phonon generation by subpicosecond laser pulses were studied experimentally and theoretically, such as ISRS, resonant stimulated Raman scattering, and displacive excitation of coherent phonons.[47–49] The two latter mechanisms rely on real optical transitions[83,84] and, therefore, are believed not to be effective in our experiment, where the central photon energy of the laser pulse $E_0 =1.54$ eV is almost twice as low as the fundamental absorption edge. The absorption coefficient for $E=1.54$ eV is 80 cm^{-1}. For the case of ISRS, the excitation of coherent phonons by laser pulses can be described in terms of the equation of motion for the normal coordinate Q of the corresponding phonon mode with an impulsive driving force.[45] This approach allows one to write the equation of motion for
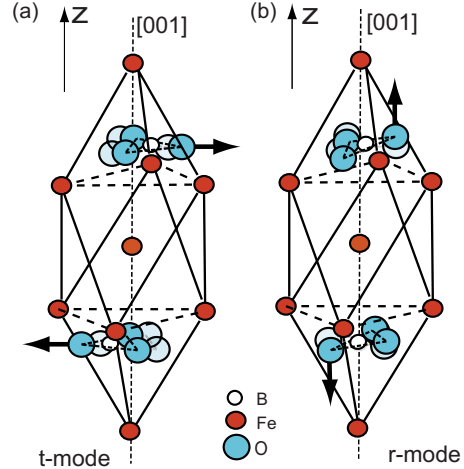

FIG. 10. (Color online) Schematic representations of the two doubly degenerate optical phonon modes E_g (Refs. 95, 98, and 99). Abbreviations *t* and *r* stand for translational and rotational modes, respectively.

TABLE II. Raman and dielectric permittivity tensor components and normal coordinates for two external doubly degenerate modes E_g.

Ω_k (THz)	Type	Normal coordinate[a] Q_k	$\mathcal{R}_{ij}$	$\delta\varepsilon_{ij}$
8.4	Translational	$Q^{t(x)}=x_1-x_2$ $Q^{t(y)}=y_1-y_2$	$xx=-yy=r_1$ $xy=yx=r_2$	$xx=-yy=r_1Q^{t(x)}$ $xy=yx=r_2Q^{t(y)}$
12.0	Rotational	$Q^{r(x)}=l_{x1}+l_{x2}$ $Q^{r(y)}=l_{y1}+l_{y2}$	$xx=-yy=r_3$ $xy=yx=r_4$	$xx=-yy=r_3Q^{r(x)}$ $xy=yx=r_4Q^{r(y)}$

[a]$x(y)_i$ denotes the shift of the ith ion complex along the $x(y)$ axis (Fig. 10). $l_{x(y)i}$ denotes the rotation of this complex with the angular momentum l along $x(y)$ axis (Ref. 99).

each mode separately.[95,100] Different from the magnon case considered above, for the phonons the normal coordinates Q represent ion displacements and, hence, obey the harmonic-oscillator equation,[48]

$$\frac{d^2Q}{dt^2}+\Omega^2Q=F(t)=\frac{1}{2}\mathcal{R}_{ij}\mathcal{E}_i(t)\mathcal{E}_j^*(t), \quad (30)$$

where $\mathcal{R}_{ij}=\partial\varepsilon_{ij}/\partial Q$ is the Raman tensor for crystals of symmetry $R\bar{3}c$ (Ref. 95) (see Table II). Ω is the frequency of the corresponding phonon mode. The normal coordinates Q for each mode observed in the experiment are listed in Table II. Note that, in contrast to the case of magnons, the normal coordinates of coherent phonons are real.

In our experiment the pump-induced rotation of the probe polarization was measured. From the symmetry properties of the dielectric permittivity tensor (Table II) it follows that only modes described by the normal coordinates $Q^{t(y)}$ and $Q^{r(y)}$ (shown in Fig. 10) can contribute to the rotation of the probe polarization (defined by off-diagonal components $\delta\varepsilon_{xy}=\delta\varepsilon_{yx}$) of the dielectric permittivity tensor.

The general solution for Eq. (30) and its main properties were extensively discussed in literature (for reviews see Refs. 48 and 49). The solution for the case of a linearly polarized pump pulse has the form

$$Q(t)\sim\mathcal{R}_{xy}I_0\sin2\theta\sin\Omega t, \quad (31)$$

where I_0 is the integrated intensity of the pump pulse and θ is the azimuthal angle of the pump polarization. The transient rotation of the probe polarization is

$$\phi(t)\sim\mathcal{R}_{xy}^2I_0\sin2\theta\sin\Omega t, \quad (32)$$

where $\mathcal{R}_{xy}=r_2$ (for the t mode $\Omega=8.4$ THz) and $\mathcal{R}_{xy}=r_4$ (for the r mode $\Omega=12.0$ THz) are the components of the Raman tensor (Table II). This theoretical dependence of the transient probe polarization rotation on the pump polarization azimuthal angle θ [inset of Fig. 9(a)] is in good agreement with our experimental data. The amplitude of the rotation ϕ_0 [Fig. 11(b)] follows a linear intensity dependence according to Eq. (32).

The temperature dependence of the frequency and, particularly, amplitude of the excited coherent phonons [Fig. 11(a)] has to be discussed in more detail. Raman scattering from phonons in $FeBO_3$ was reported by several groups.[93,94,101] In our experiment the frequencies of both observed phonon modes are independent of temperature within

the whole studied temperature range of 10–370 K. This is in good agreement with the results of previous works where no[93,94] or very weak ($\leq1\%$) (Ref. 101) shifts of the frequency with temperature were observed in the range of 10–400 K.

The change in the intensity of the Raman scattering as a function of temperature appeared to be a more intricate issue. In Ref. 93 a significant drop (by approximately a factor of 2) of the intensity of the Stokes line of the 12.0 THz phonon in $FeBO_3$ was reported. A similar, but somewhat weaker, temperature dependence was also observed for the 8.4 THz mode. This observation was considered as an indication of the influence of magnetic ordering on the phonon Raman scattering. Results published later[94] reproduced the experimental observation of Ref. 93, but the influence of magnetic order on the phonon spectra was disproved. On the other hand, in several other materials, predominantly semiconducting spinels, a magnetic-order dependent Raman scattering from phonons was observed.[102] Several mechanisms responsible for this effect were proposed.[94,103] In our experiment we did observe a change in the amplitude ϕ_0 of the 8.4 THz mode with temperature, while the amplitude of the 12.0 THz
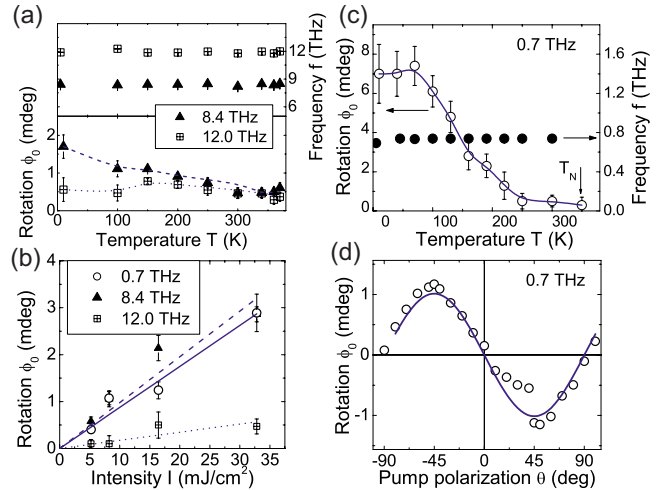

FIG. 11. (Color online) (a) Temperature dependence of the frequency f and amplitude ϕ_0 of the excited coherent phonon modes of 8.4 and 12.0 THz. (b) Dependence of the amplitude of the observed phonon modes and 0.7 THz oscillations on the pump intensity I. (c) Temperature dependence of the frequency f and amplitude ϕ_0 of the 0.7 THz oscillations. (d) Dependence of the amplitude ϕ_0 of the 0.7 THz oscillations on pump polarization θ.

mode is temperature independent within the fitting error [Fig. 11(a)]. However, no peculiarities in the temperature dependencies of both modes were observed in the vicinity of the Néel temperature, where the magnetic-order experiences drastic changes. Therefore, we conclude that the variations of ϕ_0 with temperature are not related to the changes in magnetic ordering.

2. Origin and excitation of the 0.7 THz oscillations

The origin of the 0.7 THz oscillations ought to be discussed separately. Neither Brillouin or Raman-scattering spectra[92–94,101] nor infrared-absorption spectra[96] have shown any mode with this frequency. We note that there are 27 possible optical phonon modes in FeBO$_3$ nearly half of which have been observed experimentally. Therefore, the pump-probe method used here might reveal additional features in the energy spectrum of FeBO$_3$ which were not accessible via conventional optical studies.

As can be seen from Fig. 11(c), the frequency of the 0.7 THz mode does not change in the whole range of temperatures from 10 up to 300 K where this mode is detected, following the behavior of the coherent phonon modes at 8.4 and 12.0 THz (Fig. 11), except for the variations of the amplitude ϕ_0 with temperature. This suggests that this mode is not an excitation of the spin system.

The amplitude of the oscillations, in contrast to frequency, decreases by an order of magnitude in the temperature range of 10–300 K. Above 300 K the fitting error $\Delta\phi_0$ becomes larger than the signal amplitude ϕ_0 itself. Therefore, a confident determination of the frequency above 300 K was not possible. Such a strong dependence of the amplitude on temperature and its vanishing in the vicinity of the Néel temperature $T_N = 348$ K indicates a possible relation between the observed excitation and the magnetic order.

If the observed mode itself is of nonmagnetic origin, its coupling with the magnetic order in an optical pump-probe experiment can be described by introducing the dielectric tensor components $\delta\varepsilon_{ij}(Q)$, which are functions of both the magnetic-order parameter **L** and the parameter Q, describing the medium excitation,

$$\delta\varepsilon_{ij}(Q) = \delta\varepsilon_{ij}^{(0)}(Q) + \delta K1_{ijk}(Q)M_k + \delta K2_{ijk}(Q)L_k$$
$$+ \delta b_{ijkl}(Q)L_kL_l + \delta c_{ijkl}(Q)M_kL_l\cdots, \quad (33)$$

where $\delta\varepsilon_{ij}^{(0)}(Q)$ is defined for the paramagnetic point group and describes the magnetic-order independent modulations of the dielectric tensor by the excitation Q. If $\delta\varepsilon_{ij}^{(0)}(Q) = 0$, this excitation cannot be detected in the paramagnetic phase by means of an optical measurement. $\delta K1_{ijk}(Q)$, $\delta K2_{ijk}(Q)$, $\delta b_{ijkl}(Q)$, and $\delta c_{ijkl}(Q)$ are modulations of the magneto-optical susceptibilities of different order due to the coherent phonons or some other nonmagnetic coherent medium excitation. Therefore, the latter terms in Eq. (33) describe the contributions to the modulations of the dielectric permittivity, which depend on the magnetic ordering (**M** and **L**) and can thus be detected in the magnetically ordered phase only. This can explain the decrease in the signal when the temperature is approaching the Néel temperature. On the other hand,

the Raman tensor, describing light scattering from the coherent excitation Q, is

$$\mathcal{R}_{ij} = \frac{\delta\varepsilon_{ij}}{\partial Q} = \mathcal{R}_{ij}^{(0)} + \frac{\delta K1_{ijk}}{\partial Q}M_k + \frac{K2_{ijk}}{\partial Q}L_k + \frac{\delta b_{ijkl}}{\partial Q}L_kL_l$$
$$+ \frac{\delta c_{ijkl}}{\partial Q}M_kL_l + \cdots. \quad (34)$$

If $\mathcal{R}_{ij}^{(0)} = 0$, this coherent excitation is Raman inactive and, thus, its generation via ISRS cannot occur. However, if at least one of the coefficients $\delta K1_{ijk}(Q)$, $\delta K2_{ijk}(Q)$, $\delta b_{ijkl}(Q)$, or $\delta c_{ijkl}(Q)$ is nonzero, this excitation can become Raman active in the magnetically ordered phase. Note that the amplitude of the signal drops with temperature much faster that the magnetization [Fig. 11(c)]. This might indicate that both excitation and detection of the 0.7 THz mode depend on the presence of the magnetic order. For a more detailed explanation of this excitation further thorough studies are required. We note that the excitation of this mode is sensitive not only to the presence of the magnetic ordering but also to the polarization of the pump [Fig. 11(d)]. Therefore, its observation in the experiments on the spontaneous Raman scattering requires both magnetic ordering and the proper choice of the incoming and scattered beam polarizations. This might explain why the mode with such a frequency was not, to the best of our knowledge, detected in the reported experiments on the spontaneous Raman scattering.

VII. CONCLUSIONS

The interactions of subpicosecond light pulses with the easy-plane weak ferromagnet FeBO$_3$ have been studied by means of time-resolved magneto-optical measurements. We have shown that coherent magnons can be excited by both linearly and circularly polarized laser pulses and that the microscopic mechanism of this excitation is impulsive stimulated Raman scattering. In certain experimental geometries the amplitude of the magnons excited by linearly polarized light was 2 orders of magnitude larger than of those excited by circularly polarized light, while in another geometry they were comparable. A phenomenological analysis of the excitation of magnons via ISRS showed that this difference can be explained by taking into account the strong ellipticity of the spin precession in FeBO$_3$.

We have also shown that the excitation of coherent spin precession by light pulses can be described using light-induced effective fields and the Landau-Lifshitz equation. These fields can be induced not only by circularly polarized pulses but by linearly polarized ones as well, which can be considered as ultrafast inverse Faraday and Cotton-Mouton effects, respectively. Moreover, we demonstrated that for a two-sublattice magnetic medium one has to consider two effective fields. This approach gives results which are in perfect agreement with the conclusions of the analysis based on ISRS. However, the former is convenient for the description of large light-induced changes in the magnetic system when nonlinearities in the spin motion cannot be neglected.

Excitation of two optical phonon modes was shown to occur via ISRS when the pump pulse duration is reduced to

TABLE III. The modulation of the dielectric permittivity tensor ε_{ij} by FMR and AFMR spin precessions (columns 3 and 4). Underlined are the components used in the discussion of the FMR mode excitation via ISRS. The coordinate axes x, y, and z are chosen as shown in Fig. 1. The magnetic field is assumed to be along the x axis, so that $\mathbf{L}^{(0)} \| y$, $\mathbf{M}^{(0)} \| x$.

Tensor element	FMR ($l_x, m_y, m_z \neq 0$)	AFMR ($m_x, l_y, l_z \neq 0$)	Mixed contribution
ε_{xx}^s	$b_1 l_x^2 + c_2 m_y l_x - c_3 l_x m_z$	$b_2 L_y l_y + c_1 m_x l_y + b_5 L_y l_z + c_8 M_x l_z$	0
ε_{yy}^s	$b_2 l_x^2 - c_1 m_y l_x + c_3 l_x m_z$	$b_1 L_y l_y - c_2 m_x l_y - b_5 L_y l_z - c_8 M_x l_z$	0
ε_{zz}^s	$b_3 l_x^2 - c_4 m_y l_x$	$b_3 L_y l_y + c_4 (M_x l_y + m_x l_y) + b_8 l_z^2$	0
$\underline{\varepsilon_{xy}^s}$	$\underline{(b_1 - b_2) l_x L_y} - \frac{1}{2}(c_1 + c_2)(M_x l_x - m_y L_y) + c_3 L_y m_z$	0	$b_5 l_x l_z - c_8 m_y l_z$
$\underline{\varepsilon_{xz}^s}$	$\underline{2 b_4 l_x L_y} + c_5 (m_y L_y - M_x l_x) - c_6 L_y m_z$	0	$b_6 l_x l_z - c_7 m_y l_z$
ε_{yz}^s	$b_4 l_x^2 + c_5 m_y l_x + c_6 l_x m_z$	$b_6 L_y l_z + c_7 M_x l_z$	0
ε_{xy}^a	$\underline{iK m_z}$	0	0
$\underline{\varepsilon_{xz}^a}$	$i K_1 \underline{m_y} + \underline{i K_2 l_x}$	0	0
ε_{yz}^a	0	$i K_1 m_x - i K_2 l_y$	0

40 fs. Along with this, an additional mode at 0.7 THz was observed, but its origin has not been clarified so far. The latter excitation was observed only in the magnetically ordered phase although its frequency was not sensitive to temperature changes. Therefore, it is suggested that it is a nonmagnetic excitation (coherent phonon, for example) that becomes Raman active only in a magnetically ordered state and thus can be excited via ISRS only below the Néel temperature.

APPENDIX A: DYNAMIC COMPONENTS OF THE DIELECTRIC PERMITTIVITY TENSOR

The complete expressions for the dielectric permittivity tensor components, accounting for contributions which are of first and second orders on the small spin deviations, are presented in Table III.

APPENDIX B: NORMAL COORDINATES FOR FMR MODE OF SPIN PRECESSION IN FeBO$_3$

Spin waves can be treated using the classical Hamiltonian formalism, which is one of the general methods for description of waves of various origin.[80] The Hamiltonian formalism for the magnons in the magnetic dielectric medium was developed in Ref. 81 and the application of this apparatus to the case of magnons excited by laser pulses was considered

recently in Ref. 53. Here we consider only the particular case of two-sublattice antiferromagnetic of an easy-plane type, i.e., FeBO$_3$.

The deviation of the magnetization of kth sublattice from the equilibrium can be considered in the local coordinate system, where the z_k axis is directed along the equilibrium magnetization, as shown in Fig. 12. Then, for a case of a homogenous precession, the canonical variables b_k can be introduced through the linearized Holstein-Primakoff transformation,[104]

$$b_k = \frac{M_{x_k}^k + i M_{y_k}^k}{\sqrt{2 \gamma_k \mathcal{M}_k}}, \qquad \text{(B1)}$$

where $k = 1, 2$ for the two-sublattice antiferromagnet and $\mathcal{M}_k$ and γ_k are the magnetization and the gyromagnetic ratios of the kth sublattice. $M_{x_k(y_k)}^k$ is the projection of the magnetization of the kth sublattice on the $x(y)$ axis of the kth local coordinate system. The Hamiltonian $\mathcal{H}_{\text{magnon}}$ is a quadratic function of the variables $\{b_k, b_k^*\}$. The equation of motion for these variables holds

$$i \frac{\partial b_k}{\partial t} = \frac{\partial \mathcal{H}}{\partial b_k^*}, \qquad -i \frac{\partial b_k^*}{\partial t} = \frac{\partial \mathcal{H}}{\partial b_k}, \qquad \text{(B2)}$$

where $\mathcal{H} = \mathcal{H}_{\text{magnon}} + \mathcal{H}_{\text{int}}$ and $\mathcal{H}_{\text{magnon}}$ and $\mathcal{H}_{\text{int}}$ being the Hamiltonians describing the coherent magnons and their in-
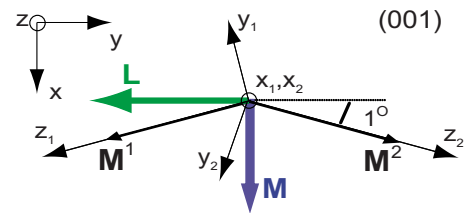

FIG. 12. (Color online) The choice of the local coordinate systems $\{x_1, y_1, z_1\}$ and $\{x_2, y_2, z_2\}$ for Eq. (B1). Note that the length of $\mathbf{L}$ and the canting of the sublattice magnetizations $\mathbf{M}^{1,2}$ are not to scale.

teraction with the electric field of light, respectively.

The Hamiltonian $\mathcal{H}_{\mathrm{magnon}}$ can be reduced to the diagonal form,

$$\mathcal{H}_{\mathrm{magnon}} = \sum_n \Omega_n Q_n Q_n^*, \tag{B3}$$

by performing the transformation from the canonical variables b_k to normal coordinates Q_n of nth eigenmode of spin precession. Q_n in this case are the classical analogs of the quantum-mechanical creation and annihilation operators[105] and satisfies the equation of motion,

$$i \frac{dQ_n}{dt} = \frac{\partial \mathcal{H}}{\partial Q_n^*}. \tag{B4}$$

The transformation is [see Eq. (12) of Ref. [53]]

$$b_k = \sum_n (u_{kn}^* Q_n - v_{kn} Q_n^*), \tag{B5}$$

where the coefficients u_{kn} and v_{kn} should satisfy the conditions that guarantee that the transformation [Eq. (B5)] is canonical and Q_n is a normal coordinate [Eqs. (8)–(11) of Ref. [53]].

For a two-sublattice antiferromagnet, possessing an easy-plane magnetic anisotropy (e.g., FeBO$_3$), the transformation $b_k \rightarrow Q_n$ holds[79]

$$b_1 + b_2 = \sqrt{\frac{\gamma H_E}{\Omega^{\mathrm{FMR}}}} (Q_{\mathrm{FMR}} - Q_{\mathrm{FMR}}^*) + \frac{1}{2} \sqrt{\frac{\Omega^{\mathrm{FMR}}}{\gamma H_E}} (Q_{\mathrm{FMR}} + Q_{\mathrm{FMR}}^*), \tag{B6a}$$

$$b_1 - b_2 = \sqrt{\frac{\gamma H_E}{\Omega^{\mathrm{AFMR}}}} (Q_{\mathrm{AFMR}} + Q_{\mathrm{AFMR}}^*) + \frac{1}{2} \sqrt{\frac{\Omega^{\mathrm{AFMR}}}{\gamma H_E}} (Q_{\mathrm{AFMR}} - Q_{\mathrm{FMR}}^*), \tag{B6b}$$

where $\Omega^{\mathrm{(A)FRM}}$ are the frequencies of the (anti)ferromagnetic modes of spin precession and $Q_{\mathrm{(A)FMR}}$ are the normal coordinates for these modes. For the FMR mode of spin precession we find that

$$b_1 + b_2 = \frac{1}{\sqrt{2\gamma \mathcal{M}_0}} (m_z + i l_x), \tag{B7}$$

where $m_z = M_{x_1}^1 + M_{x_2}^2$, $l_x = M_{y_1}^1 - M_{y_2}^2$, x and z are the axes of the general coordinate system of the sample (Fig. 7), $\mathcal{M}_0 = \mathcal{M}_1 = \mathcal{M}_2$ is the sublattice magnetization, and γ is the gyromagnetic ratio. Combining Eqs. (B6a) and (B7) we get

$$l_x = \sqrt{2\gamma \mathcal{M}_0} \sqrt{\frac{\gamma H_E}{\Omega^{\mathrm{FMR}}}} (Q_{\mathrm{FMR}} - Q_{\mathrm{FMR}}^*), \tag{B8a}$$

$$m_z = \frac{1}{2} \sqrt{2\gamma \mathcal{M}_0} \sqrt{\frac{\Omega^{\mathrm{FMR}}}{\gamma H_E}} (Q_{\mathrm{FMR}} + Q_{\mathrm{FMR}}^*), \tag{B8b}$$

which lead to the relations presented in Eqs. (7a)–(7d).

Similarly, for the AFMR mode of spin precession we find

$$b_1 - b_2 = \frac{1}{\sqrt{2\gamma \mathcal{M}_0}} (l_z + i m_x), \tag{B9}$$

where $l_z = M_{x_1}^1 - M_{x_2}^2$, $m_x = M_{y_1}^1 + M_{y_2}^2$, and x and z are the axes of the general coordinate system of the sample (Fig. 7). Therefore, the relations between the normal coordinate for this mode and the deviations of ferromagnetic and antiferromagnetic vectors are

$$l_z = \frac{1}{2} \sqrt{2\gamma \mathcal{M}_0} \sqrt{\frac{\Omega^{\mathrm{AFMR}}}{\gamma H_E}} (Q_{\mathrm{AFMR}} - Q_{\mathrm{AFMR}}^*), \tag{B10a}$$

$$m_x = \sqrt{2\gamma \mathcal{M}_0} \sqrt{\frac{\gamma H_E}{\Omega^{\mathrm{AFMR}}}} (Q_{\mathrm{AFMR}} + Q_{\mathrm{AFMR}}^*). \tag{B10b}$$

APPENDIX C: SOLUTION OF THE EQUATION OF MOTION FOR LIGHT-EXCITED MAGNONS

The solution of equation of motion for a magnon normal coordinate Q,

$$\frac{dQ}{dt} + i\Omega_0 Q = -iF(t), \tag{C1}$$

is found in a form

$$Q(t) = -ie^{-i\Omega_0 t} \int_{-\infty}^{t} dt' F(t') e^{i\Omega_0 t'}. \tag{C2}$$

The initial conditions for which we find the solution are $Q(t \rightarrow -\infty) = 0$ and $dQ/dt(t \rightarrow -\infty) = 0$. Two limiting cases are considered in this work. In the first one the driving force exerted by the laser pulse has an impulsive character $F(t) = F_0 \delta(t)$, where F_0 is an amplitude of the driving force, defined by the intensity and polarization of light and the magneto-optical permittivity, as discussed in the Sec. III [see Eq. (13)]. In this case the solution [Eq. (C2)] has a form

$$Q(t) = -iF_0 e^{-i\Omega_0 t} = -F_0(i \cos \Omega_0 t + \sin \Omega_0 t). \tag{C3}$$

As an example, we consider the circularly polarized pulse propagating along the z axis. Then

$$F_0 = \mp \frac{I_0}{8nc} K b_z \tag{C4}$$

and

$$Q(t) = \pm \frac{I_0}{8nc} K b_z (\sin \Omega_0 t + i \cos \Omega_0 t), \tag{C5}$$

which corresponds to Eq. (15a). The consideration for the linearly polarized light is analogous. The resulting expression for the normal coordinate differs in phase from Eq. (C5) by $\pi/2$ because the product $e_i e_j^*$ in the expression for the driving force F_0 is imaginary for the circularly polarized light and is real for the linearly polarized one.

In the limiting case of an absorptive medium the light exerts a quasistationary driving force approximated by the Heaviside step function,

$$F(t) = \begin{cases} F_0' + iF_0'', & t > 0 \\ 0, & t < 0, \end{cases}$$

where we do not make any assumption about the origin of this force. Then the solution [Eq. (C2)] of the equation of motion is

$$Q(t) = F_0' \frac{\cos \Omega_0 t - i \sin \Omega_0 t - 1}{\Omega_0}$$

$$+ iF_0'' \frac{\cos \Omega_0 t - i \sin \Omega_0 t - 1}{\Omega_0}. \quad (C6)$$

Assuming that $iF(t)$ is real, i.e., $F_0' = 0$, $F_0'' \neq 0$, we obtain Eq. (20a) and, consequently,

$$m_z(t) = 2F_0'' b_z \frac{\sin \Omega_0 t}{\Omega_0},$$

$$l_x(t) = 2F_0'' a_x \frac{[1 - \cos \Omega_0 t]}{\Omega_0}. \quad (C7)$$

Otherwise the time dependences of m_z and l_z are the opposite. The term $\sim \cos \Omega_0 t$ does not appear in both cases, in contrast to the impulsive excitation.

APPENDIX D: LIGHT-INDUCED EFFECTIVE FIELDS AND TORQUES

As an example of derivation of light-induced fields we consider the case of light propagating along the z axis. First, we obtain the expressions for the circularly polarized light. The relevant dielectric permittivity tensor component is

$$\delta \varepsilon_{xy}^a = iK m_z. \quad (D1)$$

The Hamiltonian describing the interaction of a short circularly polarized laser pulse with the medium is

$$\mathcal{H}_{\text{int}}^{\sigma^\pm} = \frac{1}{16\pi} \varepsilon_{xy}^a \mathcal{E}_x(t) \mathcal{E}_y^*(t) = \pm \frac{I_0}{8nc} K m_z \delta(t), \quad (D2)$$

where $\mathcal{E}_{x(y)}(t)$ are the time-dependent $x(y)$ components of the electric field of light.

Therefore there is only "ferromagnetic" effective field induced by such a pulse,

$$\mathbf{H}^{\text{eff},\sigma^\pm} = -\frac{\partial \mathcal{H}_{\text{int}}^{\sigma^\pm}}{\partial \mathbf{m}} = \mp \frac{I_0}{8nc} K \delta(t) \hat{z}, \quad (D3a)$$

$$\mathbf{h}^{\text{eff},\sigma^\pm} = -\frac{\partial \mathcal{H}_{\text{int}}^{\sigma^\pm}}{\partial \mathbf{l}} = 0. \quad (D3b)$$

Then, taking into account the equilibrium orientation of ferromagnetic and antiferromagnetic vectors ($\mathbf{M} \| x, \mathbf{L} \| y$) we find that the torque created by the light-induced effective field $\mathbf{H}^{\text{eff},\sigma^\pm}$ is

$$\frac{d\mathbf{m}}{dt} = -\gamma \mathbf{M} \times \mathbf{H}^{\text{eff},\sigma^\pm}$$

$$= -\gamma (M_x \cdot H_z^{\text{eff},\sigma^\pm}) \hat{y}$$

$$= \pm \gamma \frac{I_0}{8nc} K M_x^{(0)} \delta(t) \hat{y}, \quad (D4a)$$

$$\frac{d\mathbf{l}}{dt} = -\gamma \mathbf{L} \times \mathbf{H}^{\text{eff},\sigma^\pm}$$

$$= -\gamma (L_y \cdot H_z^{\text{eff},\sigma^\pm}) \hat{x}$$

$$= \pm \gamma \frac{I_0}{8nc} K L_y^{(0)} \delta(t) \hat{x}. \quad (D4b)$$

Therefore, circularly polarized pulses propagating along the z axis create the torque that moves the spins in the xy plane.

Interaction of linearly polarized pulses propagating along the z axis is described by (see Table III)

$$\varepsilon_{xx}^s = b_2 L_y^{(0)2} + c_1 M_x^{(0)} L_y^{(0)} + (b_5 L_y^{(0)} + c_8 M_x^{(0)}) l_z, \quad (D5a)$$

$$\varepsilon_{yy}^s = b_1 L_y^{(0)2} - c_2 M_x^{(0)} L_y^{(0)} - (b_5 L_y^{(0)} + c_8 M_x^{(0)}) l_z, \quad (D5b)$$

$$\delta \varepsilon_{xy}^s = (b_1 - b_2) l_x L_y - \frac{1}{2}(c_1 + c_2)(M_x l_x - m_y L_y) + c_3 L_y m_z. \quad (D5c)$$

The Hamiltonian is

$$\mathcal{H}_{\text{int}}^{\text{lin}} = \frac{I_0 \delta(t)}{4nc} \Bigg[(b_2 L_y^{(0)2} + c_1 M_x^{(0)} L_y^{(0)}) \cos^2 \theta$$

$$+ (b_1 L_y^{(0)2} - c_2 M_x^{(0)} L_y^{(0)}) \sin^2 \theta + \frac{1}{2} \bigg((b_1 - b_2) l_x L_y^{(0)}$$

$$- \frac{1}{2}(c_1 + c_2)(M_x^{(0)} l_x - m_y L_y^{(0)}) + c_3 L_y^{(0)} m_z \bigg) \sin 2\theta$$

$$+ (b_5 L_y^{(0)} + c_8 M_x^{(0)}) l_z \cos 2\theta \Bigg]. \quad (D6)$$

The light-induced effective fields in this case are

$$\mathbf{H}^{\text{eff,lin}} = -\frac{\partial \mathcal{H}_{\text{int}}^{\text{lin}}}{\partial \mathbf{M}} = -\frac{I_0 \delta(t)}{4nc} \Bigg[(c_1 \cos^2 \theta - c_2 \sin^2 \theta) L_y^{(0)} \hat{x}$$

$$- \frac{1}{4}(c_1 + c_2) L_y^{(0)} \sin 2\theta \hat{y} + \frac{1}{2} c_3 \sin 2\theta L_y^{(0)} \hat{z} \Bigg], \quad (D7a)$$

$$\mathbf{h}^{\text{eff,lin}} = -\frac{\partial \mathcal{H}_{\text{int}}^{\text{lin}}}{\partial \mathbf{L}}$$

$$= \frac{I_0 \delta(t)}{4nc} \Bigg\{ \frac{1}{2} \bigg[(b_1 - b_2) L_y^{(0)} - \frac{1}{2}(c_1 + c_2) M_x^{(0)} \bigg] \sin 2\theta \hat{x}$$

$$+ [(b_2 \cos^2 \theta + b_1 \sin^2 \theta) L_y^{(0)}$$

$$+ (c_1 \cos^2 \theta - c_2 \sin^2 \theta) M_x^{(0)}] \hat{y}$$

$$+ [b_5 L_y^{(0)} + c_8 M_x^{(0)}] \cos 2\theta \hat{z} \bigg\}. \quad \text{(D7b)}$$

Only the components H_z, H_y, and h_x of these fields can lead to an excitation of the FMR mode of the spin precession. Therefore, the torques exerted by the linearly polarized pulse propagating along the z axis are

$$\frac{d\mathbf{m}}{dt} = -\gamma[\mathbf{M} \times \mathbf{H}^{\text{eff,lin}} + \mathbf{L} \times \mathbf{h}^{\text{eff,lin}}]$$

$$= -\gamma[(M_x^{(0)} \cdot H_z^{\text{eff,lin}})\hat{y} + (M_x^{(0)} \cdot H_y^{\text{eff,lin}} + L_y^{(0)} \cdot h_x^{\text{eff,lin}})\hat{z}]$$

$$\cong \gamma \frac{I_0 \delta(t)}{8nc}(b_1 - b_2)L^{(0)2} \sin 2\theta \hat{z}, \quad \text{(D8)}$$

where we took into account that $M_x \ll L_y$. There is also the torque

$$\frac{d\mathbf{l}}{dt} = -\gamma(L_y^{(0)} \cdot H_z^{\text{eff,lin}})\hat{x} = \gamma \frac{I_0 \delta(t)}{8nc} c_3 L^{(0)2} \sin 2\theta \hat{x}, \quad \text{(D9)}$$

however, as discussed in Sec. V C, the amplitude of the precession caused by a torque directed in the xy plane is 2 orders of magnitude smaller that of the one caused by a torque along the z axis [Eq. (D8)]. Therefore, the linearly polarized pulses propagating along the z axis excite the spin precession because of the light-induced effective field $\mathbf{h}^{\text{eff,lin}} \| x$.

[1] J. Stöhr and H. C. Siegmann, *Magnetism from Fundamentals to Nanoscale Dynamics* (Springer-Verlag, Berlin, Heidelberg, 2006).

[2] E. Beaurepaire, J.-C. Merle, A. Daunois, and J.-Y. Bigot, Phys. Rev. Lett. **76**, 4250 (1996).

[3] G. P. Zhang and W. Hübner, Phys. Rev. Lett. **85**, 3025 (2000).

[4] H. Regensburger, R. Vollmer, and J. Kirshner, Phys. Rev. B **61**, 14716 (2000).

[5] B. Koopmans, M. van Kampen, J. T. Kohlhepp, and W. J. M. de Jonge, Phys. Rev. Lett. **85**, 844 (2000).

[6] E. Beaurepaire, M. Maret, V. Halté, J.-C. Merle, A. Daunois, and J.-Y. Bigot, Phys. Rev. B **58**, 12134 (1998).

[7] J. Hohlfeld, E. Matthias, R. Knorren, and K. H. Bennemann, Phys. Rev. Lett. **78**, 4861 (1997).

[8] A. V. Kimel, R. V. Pisarev, J. Hohlfeld, and Th. Rasing, Phys. Rev. Lett. **89**, 287401 (2002).

[9] L. Guidoni, E. Beaurepaire, and J.-Y. Bigot, Phys. Rev. Lett. **89**, 017401 (2002).

[10] E. Beaurepaire, G. M. Turner, S. M. Harel, M. C. Beard, J.-Y. Bigot, and C. A. Schmuttenmaer, Appl. Phys. Lett. **84**, 3465 (2004).

[11] M. Vomir, L. H. F. Andrade, E. Beaurepaire, M. Albrecht, and J.-Y. Bigot, J. Appl. Phys. **99**, 08A501 (2006).

[12] F. Dalla Longa, J. T. Kohlhepp, W. J. M. de Jonge, and B. Koopmans, Phys. Rev. B **75**, 224431 (2007).

[13] A. V. Kimel, A. Kirilyuk, A. Tsvetkov, R. V. Pisarev, and Th. Rasing, Nature (London) **429**, 850 (2004).

[14] G. Ju, J. Hohlfeld, B. Bergman, R. J. M. van de Veerdonk, O. N. Mryasov, J. Y. Kim, X. Wu, D. Weller, and B. Koopmans, Phys. Rev. Lett. **93**, 197403 (2004).

[15] A. Melnikov, I. Radu, U. Bovensiepen, O. Krupin, K. Starke, E. Matthias, and M. Wolf, Phys. Rev. Lett. **91**, 227403 (2003).

[16] J. Zhao, A. V. Bragas, D. J. Lockwood, and R. Merlin, Phys. Rev. Lett. **93**, 107203 (2004).

[17] G. Ju, A. V. Nurmikko, R. F. C. Farrow, R. F. Marks, M. J. Carey, and B. A. Gurney, Phys. Rev. Lett. **82**, 3705 (1999).

[18] M. van Kampen, B. Koopmans, J. T. Kohlhepp, and W. J. M. de Jonge, J. Magn. Magn. Mater. **240**, 291 (2002).

[19] M. van Kampen, C. Jozsa, J. T. Kohlhepp, P. LeClair, L. Lagae, W. J. M. de Jonge, and B. Koopmans, Phys. Rev. Lett. **88**, 227201 (2002).

[20] Q. Zhang, A. V. Nurmikko, A. Anguelouch, G. Xiao, and A. Gupta, Phys. Rev. Lett. **89**, 177402 (2002).

[21] F. Hansteen, A. V. Kimel, A. Kirilyuk, and Th. Rasing, Phys. Rev. Lett. **95**, 047402 (2005).

[22] S. Tomimoto, M. Matsubara, T. Ogasawara, H. Okamoto, T. Kimura, and Y. Tokura, Phys. Rev. Lett. **98**, 017402 (2007).

[23] A. V. Kimel, A. Kirilyuk, P. A. Usachev, R. V. Pisarev, A. M. Balbashov, and Th. Rasing, Nature (London) **435**, 655 (2005).

[24] F. Hansteen, A. Kimel, A. Kirilyuk, and Th. Rasing, Phys. Rev. B **73**, 014421 (2006).

[25] C. D. Stanciu, F. Hansteen, A. V. Kimel, A. Tsukamoto, A. Itoh, A. Kirilyuk, and Th. Rasing, Phys. Rev. Lett. **98**, 207401 (2007).

[26] C. D. Stanciu, F. Hansteen, A. V. Kimel, A. Kirilyuk, A. Tsukamoto, A. Itoh, and T. Rasing, Phys. Rev. Lett. **99**, 047601 (2007).

[27] W. Hübner and G. P. Zhang, Phys. Rev. B **58**, R5920 (1998).

[28] R. Gómez-Abal, O. Ney, K. Satitkovitchai, and W. Hübner, Phys. Rev. Lett. **92**, 227402 (2004).

[29] P. M. Oppeneer and A. Liebsch, J. Phys.: Condens. Matter **16**, 5519 (2004).

[30] B. Koopmans, J. J. M. Ruigrok, F. Dalla Longa, and W. J. M. de Jonge, Phys. Rev. Lett. **95**, 267207 (2005).

[31] C. A. Perroni and A. Liebsch, Phys. Rev. B **74**, 134430 (2006).

[32] G. Lefkidis and W. Hübner, Phys. Rev. B **76**, 014418 (2007).

[33] U. Atxitia, O. Chubykalo-Fesenko, N. Kazantseva, D. Hinzke, U. Nowak, and R. W. Chantrell, Appl. Phys. Lett. **91**, 232507 (2007).

[34] N. Kazantseva, U. Nowak, R. W. Chantrell, J. Hohlfeld, and A. Rebei, Europhys. Lett. **81**, 27004 (2008).

[35] F. Meier and B. P. Zakharchenya, *Optical Orientation* (Elsevier, New York, 1984).

[36] G. Ju, A. Vertikov, A. V. Nurmikko, C. Canady, Gang Xiao R. F. C. Farrow, and A. Cebollada, Phys. Rev. B **57**, R700 (1998).

[37] L. P. Pitaevskii, Sov. Phys. JETP **12**, 1008 (1961).

[38] P. S. Pershan, Phys. Rev. **130**, 919 (1963).

[39] J. P. van der Ziel, P. S. Pershan, and L. D. Malmstrom, Phys. Rev. Lett. **15**, 190 (1965).

[40] B. A. Zon, V. Ya. Kupershmidt, G. V. Pakhomov, and T. T. Urazbaev, JETP Lett. **45**, 273 (1987).

[41] V. N. Gridnev, R. V. Pisarev, S. I. Shablaev, and M. G. Khalmu-

ratov, Sov. Phys. Solid State **30**, 1951 (1988).

[42] Y. R. Shen and N. Bloembergen, Phys. Rev. **143**, 372 (1966).

[43] Y. R. Shen and N. Bloembergen, Phys. Rev. **137**, A1787 (1965).

[44] K. A. Nelson, R. J. D. Miller, D. R. Lutz, and M. D. Fayer, J. Appl. Phys. **53**, 1144 (1982).

[45] Y.-X. Yan, E. B. Gamble, Jr., and K. A. Nelson, J. Chem. Phys. **83**, 5391 (1985).

[46] Y.-X. Yan and K. A. Nelson, J. Chem. Phys. **87**, 6240 (1987); **87**, 6257 (1987).

[47] L. Dhar, J. A. Rogers, and K. A. Nelson, Chem. Rev. (Washington, D.C.) **94**, 157 (1994).

[48] R. Merlin, Solid State Commun. **102**, 207 (1997).

[49] T. Dekorsy, G. C. Cho, and H. Kurz, in *Light Scattering in Solids VIII*, edited by M. Cardona and G. Güntherodt (Springer, Berlin, 2000).

[50] J.-C. Diels and W. Rudolph, *Ultrashort Laser Pulse Phenomena*, 2nd ed. (Academic, Amsterdam, 2006).

[51] T. E. Stevens, J. Kuhl, and R. Merlin, Phys. Rev. B **65**, 144304 (2002).

[52] A. M. Kalashnikova, A. V. Kimel, R. V. Pisarev, V. N. Gridnev, A. Kirilyuk, and T. Rasing, Phys. Rev. Lett. **99**, 167205 (2007).

[53] V. N. Gridnev, Phys. Rev. B **77**, 094426 (2008).

[54] I. Bernal, C. W. Struck, and J. G. White, Acta Crystallogr. **16**, 849 (1963).

[55] Here we define ellipticity of the spin precession as the ratio between out-of-plane and in-plane deviations of spins. By the strong ellipticity we mean that the in-plane deviation is much larger than the out-of-plane one.

[56] E. Burzo, in *Numerical Data and Functional Relations*, Landolt-Börnstein, New Series, Group III, Vol. 27H (Springer-Verlag GmbH, Berlin, 1993).

[57] A. S. Borovik-Romanov and N. M. Kreines, Phys. Rep. **81**, 351 (1982).

[58] J. Schober, IEEE Trans. Magn. **12**, 401 (1976).

[59] R. Diehl, Solid State Commun. **17**, 743 (1975).

[60] B. Andlauer, O. F. Schirmer, and J. Schneider, Solid State Commun. **13**, 1655 (1973).

[61] E. A. Turov, *Physical Properties of Magnetically Ordered Crystals* (Academic, New York, London, 1965).

[62] All values of the effective fields are given for room temperature according to Ref. 58 and references therein.

[63] I. Dzyaloshinsky, J. Phys. Chem. Solids **4**, 241 (1958).

[64] T. Moriya, Phys. Rev. **120**, 91 (1960).

[65] A. J. Kurtzig, R. Wolfe, R. C. LeCraw, and J. W. Nielsen, Appl. Phys. Lett. **14**, 350 (1969).

[66] L. Landau and E. Lifshitz, Phys. Z. Sowjetunion **8**, 153 (1935).

[67] E. A. Turov, A. V. Kolchanov, V. V. Men'shenin, I. F. Mirsaev, and V. V. Nikolaev, *Symmetry and Physical Properties of Antiferromagnets* (Fizmatlit, Moscow, 2001) (in Russian).

[68] E. A. Turov and N. G. Guseĭnov, Sov. Phys. JETP **11**, 955 (1960).

[69] W. Jantz, J. R. Sandercock, and W. Wettling, J. Phys. C **9**, 2229 (1976).

[70] R. C. LeCraw, R. Wolfe, and J. W. Nielsen, Appl. Phys. Lett. **14**, 352 (1969).

[71] S. G. Ovchinnikov and V. N. Zabluda, J. Exp. Theor. Phys. **98**, 135 (2004).

[72] P. A. Markovin, R. V. Pisarev, A. M. Kalashnikova, and Th. Rasing, JETP Lett. **86**, 712 (2007).

[73] R. V. Pisarev, Sov. Phys. JETP **31**, 761 (1970).

[74] L. D. Landau, E. M. Lifshitz, and L. P. Pitaevskii, *Landau and Lifshitz Course of Theoretical Physics, Electrodynamics of Continuous Media* (Elsevier, Oxford, 2006), Vol. 8.

[75] A. K. Zvezdin and V. A. Kotov, *Modern Magneto-Optics and Magneto-Optical Materials* (IOP, London, 1997).

[76] R. Wolfe, A. J. Kurtzig, and R. C. LeCraw, J. Appl. Phys. **41**, 1218 (1970).

[77] G. A. Smolenskiĭ, R. V. Pisarev, and I. G. Siniĭ, Sov. Phys. Usp. **18**, 410 (1975).

[78] J. Ferré and G. A. Gehring, Rep. Prog. Phys. **47**, 513 (1984).

[79] V. S. Lutovinov and V. L. Safonov, Sov. Phys. Solid State **22**, 1541 (1980).

[80] V. E. Zakharov and E. A. Kuznetsov, in *Soviet Scientific Reviews*, Mathematical Physics Reviews, edited by S. P. Novikov (OPA, Amsterdam, 1984), Sec. C; Phys. Usp. **40**, 1087 (1997).

[81] V. S. L'vov, *Nonlinear Spin Waves* (Nauka, Moscow, 1987) (in Russian).

[82] Y. R. Shen, *Principles of Nonlinear Optics* (Willey, New York, 1984).

[83] G. A. Garrett, T. F. Albrecht, J. F. Whitaker, and R. Merlin, Phys. Rev. Lett. **77**, 3661 (1996).

[84] H. J. Zeiger, J. Vidal, T. K. Cheng, E. P. Ippen, G. Dresselhaus, and M. S. Dresselhaus, Phys. Rev. B **45**, 768 (1992).

[85] A. V. Kimel, A. Kirilyuk, and Th. Rasing, Laser Photonics Rev. **1**, 275 (2007).

[86] S. R. Woodford, A. Bringer, and S. Blügel, J. Appl. Phys. **101**, 053912 (2007).

[87] As one can see in Figs. 3(b) and 5(a), there is an offset of the oscillations from the zero line that decays on long-time scales. This shift is of a nonmagnetic origin because it does not depend on the applied magnetic field. From Figs. 3(b) and 5(a) one can see, moreover, that this shift is present even for polarizations of pump and probe beams that show no spin precession oscillations. We attribute this shift to optically induced birefringence and, hence, omit it from the discussion of the experimental results.

[88] R. M. White, R. J. Nemanich, and C. Herring, Phys. Rev. B **25**, 1822 (1982); A. P. Cracknell, J. Phys. C **2**, 500 (1969).

[89] A. V. Kimel, A. Kirilyuk, F. Hansteen, R. V. Pisarev, and Th. Rasing, J. Phys.: Condens. Matter **19**, 043201 (2007).

[90] P. S. Pershan, J. P. van der Ziel, and L. D. Malmstrom, Phys. Rev. **143**, 574 (1965).

[91] In simulations the 150 fs effective-field pulse induced by linearly [h_x^{eff}, Eq. (27d)] or circularly [H_z^{eff}, Eq. (27a)] polarized lights was inserted in the LL equations (B). The light-induced effective-field value was taken as 1 kG for both linearly and circularly polarized pulses, the applied magnetic-field value was 1 kG, and the exchange, Dzyaloshinsky, and anisotropy fields values were taken from Ref. 58.

[92] W. Wettling, W. D. Wilber, and C. E. Patton, J. Appl. Phys. **53**, 8163 (1982).

[93] I. W. Shepherd, Phys. Rev. B **5**, 4524 (1972); J. Appl. Phys. **42**, 1482 (1971).

[94] A. E. Meixner, R. E. Dietz, and D. L. Rousseau, Phys. Rev. B **7**, 3134 (1973).

[95] K. Nakamoto, *Infrared and Raman Spectra of Inorganic and Coordination Compounds* (Wiley, New York, 1986).

[96] K. Wakamura, T. Okuda, and T. Tsushima, Opt. Commun. **23**, 249 (1977).

[97] K. Parlinski, J. Łażewski, P. T. Jochym, A. Chumakov, R.

Rüffer, and G. Kresse, Europhys. Lett. **56**, 275 (2001).

[98] I. Nakagawa and J. L. Walter, J. Chem. Phys. **51**, 1389 (1969).

[99] S. Bhagavantam and T. Venkatarayudu, *Theory of Groups and Its Applications to Physical Properties* (Academic, New York, 1969).

[100] W. Hayes and R. Loudon, *Scattering of Light by Crystals* (Wiley, New York, 1978).

[101] N. Koshizuka, T. Ocuda, U. Udagawa, and T. Tsushima, J. Phys. Soc. Jpn. **37**, 354 (1974).

[102] E. F. Steigmeier and G. Harbeke, Phys. Kondens. Mater. **12**, 1 (1970).

[103] N. Suzuki and H. Kamimura, Solid State Commun. **11**, 1603 (1972); J. Phys. Soc. Jpn. **35**, 985 (1973).

[104] T. Holstein and H. Primakoff, Phys. Rev. **58**, 1098 (1940).

[105] A. I. Akhiezer, V. G. Bar'yakhtar, and S. V. Peletminskii, *Spin Waves* (North-Holland, Amsterdam, 1968).